scientific reports

Check for updates

OPEN

Multiple subcortical and subcortico–cortico dynamic network reconfigurations characterize focal-to-bilateral tonic–clonic seizures

Shilpi Modi[1], A. Ankeeta[1], Walter Hinds[1], Michael R. Sperling[1], Xiaosong He[2] & Joseph I. Tracy[1,3]✉

Temporal lobe epilepsy (TLE) is the most common focal epilepsy, with focal to bilateral tonic–clonic seizures (FBTCS+) a more severe form of the disorder. Evidence has underscored the critical role of the thalamus, mesial temporal region, basal ganglia and cerebellum, along with the cortex, in the propagation, termination, and modulation of seizure activity. We examined time variant patterns of interaction within and between 7 cortical and 4 subcortical systems in 55 healthy controls and 56 patients with TLE (n = 40 with FBTCS+ and 15 without), isolating those patterns most distinctive of FBTCS+ utilizing tools from dynamic network neuroscience on inter-ictal resting state fMRI data. A complex set of subcortio-cortico interactions appeared to support the secondary generalization characteristic of FBTCS+ status, specifically integrations involving the caudate and cereb-5 subcortical subsystems with the ventral attention network, suggesting motor and attention system communications are dysregulated. These abnormal subcortico–cortico dynamics were more prominent in current versus a remote history of FBTCS+. We concluded that the inter-ictal state provided a breeding ground for reconfiguring dynamic communication within and between multiple cortical-subcortical systems. These findings broaden our understanding of seizure propagation effects in TLE, pointing toward biomarkers that may mark the transition from focal seizures to the more severe form of TLE (FBTCS +).

Keywords Temporal lobe epilepsy, Resting state dynamics, Subcortico–cortico interactions, Focal-to-bilateral tonic clonic seizures, Functional MRI

Epilepsy can be a chronic disorder characterized by recurrent seizures. The recurrence is marked by regional abnormalities that initiate the seizure, as well as abnormalities in the structural and functional pathways that propagate and spread the seizure activity elsewhere in the brain[1]. Identifying not just the ictal source in the brain, but also these additional more distal abnormalities, will likely be important for designing individualized therapeutics[2], predicting treatment response, and assessing the patient's capacity to recover from seizure's harmful effects. Temporal lobe epilepsy (TLE) is the most common focal epilepsy syndrome in adults, and a more severe form of the disorder involves seizures that secondarily generalize (i.e., focal to bilateral tonic–clonic seizures; such focal TLE patients to be referred to as FBTCS +), with this affecting at least a third of drug resistant TLE patients[3–5]. FBCTS+ has been associated with lower overall quality of life[6] and is a predictor of unfavorable postsurgical outcomes[7–9]. FBTCS+ is also a major risk factor for seizure-related injuries[10] and sudden unexpected death in epilepsy (SUDEP)[11,12]. FBTCS+ patients display more neurocognitive deficits than focal TLE patients without FBTCS (to be referred to as FBTCS–)[13,14]. FBTCS+ may also have a distinct clinical history, differing on features such as age of onset of epilepsy[15]. Methods for early identification of focal TLE

[1]Department of Neurology, Comprehensive Epilepsy Centre, Thomas Jefferson University, Philadelphia, PA, USA. [2]Department of Psychology, University of Science and Technology of China, Hefei, Anhui, People's Republic of China. [3]Departments of Neurology and Radiology, Director, Clinical Brain Mapping and Cognitive Neuroscience Laboratory, Sidney Kimmel Medical College, Thomas Jefferson University, 901 Walnut Street, Suite 447, Philadelphia, PA 19107, USA. ✉email: joseph.tracy@Jefferson.edu

patients at risk for FBTCS+ would represent a significant clinical advance, as would techniques that identify the specific brain regional connectivities involved in the extra-temporal structures and pathways that implement FBTCS activity. In essence, the reason why some and not other focal TLE patients experience FBTCS remains poorly understood.

Three patterns of abnormal subcortico–cortico communication have emerged as important characteristics of TLE generally, and for FBTCS+ patients in particular. First, abnormalities in structural and functional connectivity involving the thalamus have been demonstrated in focal TLE, with convergent evidence underscoring the critical role of the thalamus in interaction with other circuits during FBTCS activity[5,16]. Compared to patients with focal seizures only, FBTCS+ patients present with additional thalamic atrophy[17,18] and greater disruptions to structural[9,19] and functional[20,21] thalamocortical connectivity. The thalamus may act as a key driver for the extension of epileptogenic networks beyond the temporal lobe[22]. The mechanism for this is thought to involve the synchronization of abnormal cortical–subcortical electrical discharges and the loss of thalamic inhibition[16,22–24], which cause the ictal signal to propagate to widespread cortical areas[25].

Abnormalities in structural and functional connectivity involving the basal-ganglia have also been shown in focal TLE, and, again, such abnormalities appear more pronounced in FBTCS+. The basal ganglia (BG) are a complex group of nuclei[26], that serve as a 'braking system' between the cortex and thalamus[1]. BG interact with the thalamus and cortex via several parallel circuits including the direct and indirect pathways[27,28]. The BG have been shown to be hyperactive during FBTCS+[29], and TLE patients with FBTCS+ display additional BG atrophy compared to patients with focal only seizures[18]. Work from our lab has demonstrated that disruption of thalamic/basal ganglia circuitry (connectivity) is a unique feature of FBTCS+, with such disruptions causing a breakdown in normal patterns of inhibition, allowing the spread of epileptic activity to cortex[5]. A large body of experimental and clinical evidence suggests an anti-convulsive role for the BG during temporal lobe seizures is accomplished via feedback pathways to the cortex[30]. A stereo-electroencephalographic study has reported changes in cortical–striatum synchronization as a part of an endogenous mechanism controlling the duration and termination of abnormal oscillations within the striato-thalamo-cortical loop, pointing to an important element in the propagation of the temporal lobe ictal signals[31].

Another subcortical system of emerging importance for our understanding of seizure generalization is the cerebellum[24,32]. Here again, TLE patients with FBTCS+ show more pronounced abnormalities. A recent study showed gray matter volume reduction in FBCTS+ patients in bilateral cortical structures, head of caudate, the thalamus, as well as the cerebellum[33]. These reductions were associated with disease duration. Cerebral blood flow (CBF) increases have been found in the cerebellum during generalization as well as post-ictally, with these increases prominent in the midbrain and thalamus. This study also noted a relationship with cortex, as these CBF increases in the cerebellum correlated with CBF decreases in fronto-parietal association cortex[29]. The authors postulated that the increased cerebellar activity may contribute to seizure termination and/or to post-ictal suppression[34].

As evidence regarding the role of thalamo-striato-cerebellar circuitry in FBTCS+ grows[2,24,35], an important question to ask is whether FBTCS patients necessarily possess abnormality and disruption in the connectivity of *ALL* of these subcortical systems, and, if so, whether the abnormalties in one system correlates with the abnormality in others. An important observation with regard to these prior investigations is that they all largely focused on the status of a single subcortical system, yielding little evidence about their comparative impact on cortex, and leaving open questions about whether cortical effects arise from each system independently or whether the systems act in a coordinated fashion.

Another feature of these prior studies is that they all focused on the static aspects of regional connectivity. It remains possible, for instance, that subcortico–cortico abnormalities in TLE, and specifically within FBTCS+, involve changes in the temporal dynamics of these systems such that there is a time varying loss (or increase) in communication within a subcortical system, or between a particular subcortical system and cortex. As a complex system, the human brain's modular structure has been shown not to be static, but prone to undergo changes in regional communication patterns in response to both internal and external drivers such as disease[36]. Importantly, measures of dynamic functional connectivity have been shown to be effective in identifying neurodegenerative processes and have shown potential as diagnostic and prognostic biomarkers for diseases[37], including epilepsy[38–40].

In accord with all the above, in this project, we argue that interrogating the dynamics of multiple subcortical systems, and testing for distinct subcortico–cortico interactions will broaden our understanding of seizure propagation effects in TLE as a whole and FBTCS, in particular. Specifically, we sought to answer two questions. First, compared to healthy participants (HPs), does TLE as a whole, or subgroups with FBTCS activity (FBTCS+ patients with current [past year] or remote (beyond 12 months), referred to as FBTCS+ current, FBTCS+ remote, respectively) demonstrate abnormal dynamic functional connectivity (dFC) within all four subcortical systems (thalamic, striatal, mesial temporal, cerebellar) and across all types of subcortical-cortical interactions. Second, are any of the abnormalities observed linked or associated, raising the possibility that these systems do not operate independently in their implementation of FBTCS activity.

To accomplish these goals, we pursued a comprehensive characterization of tonic, baseline resting state dFC in left TLE. Distinct from previous investigations[15,20,21,41], we utilized measures of dFC focused on multiple intrinsic subcortical systems (thalamic, striatal, mesial temporal, cerebellar) and their interaction with seven well-established intrinsic cortical systems (visual, somatomotor, dorsal attention network, ventral attention network, limbic, control and default mode network)[42]. We included the mesial temporal network as a subcortical system because of its clear role in temporal lobe seizures[15,43,44]. Accordingly, we suspected that FBCTS- and FBTCS+ LTLE patients will have similar patterns of dFC for the mesial temporal system.

In line with our prior work demonstrating the effectiveness of resting state functional networks for the identification of seizure impact on intrinsic brain systems[45], we acquired resting state functional MRI data from

LTLE patients and matched HPs. Time series of the BOLD response were extracted from 200 cortical regions[46], 54 subcortical regions (Melbourne subcortical atlas[47]), and seven cerebellar parcellations[48] in each participant. Using a sliding-window strategy, we generated cross-region coherence matrices over time. We then applied dynamic network analysis methods to detect community structures over time[49] and quantified subcortico–cortico network reconfigurations (Fig. 1). We focused on the dynamic measures of 'recruitment' (the probability of intra-communication with peer regions from the same subsystem), 'flexibility' (frequency with which a region changes its assigned community over time) and 'integration' (probability of inter-communication with regions from other subsystems)[50,51].

Due to the high dimensionality of the feature sets emerging for our dFC measures, we first undertook a feature reduction step using Repeated Measures Multiple Analysis of Variance (rmMANOVA) comparisons to determine which dFC features were abnormal in focal LTLE as a whole (LTLE versus matched HPs), or uniquely associated with the status of one of our subgroups (FBTCS−, FBTCS+ current, FBTCS+ remote). Next, for feature ranking and group discrimination, we brought the significant results of the rmMANOVA's into the competitive context of random forest (RF) classification, allowing us to determine the dFC metrics that best discriminated between FBTCS+ and FBTCS− (also between current and remote FBTCS +). The RF models ranked the variable importance of the dFC measures in terms of their classification success. Lastly, based upon the RF findings we tested for group differences in the associations among the dFC metrics to determine if they were abnormally linked or showed dependencies within FBTCS+ or the FBTCS+ subgroups.

We hypothesized that our dFC metrics would reveal abnormalities in subcortico–cortico interactions (communication) in LTLE as a whole. However, given the evidence that FBTCS activity puts patients at risk for wide spread brain dysfunction, we hypothesized that only the FBTCS+ group would display disruptions
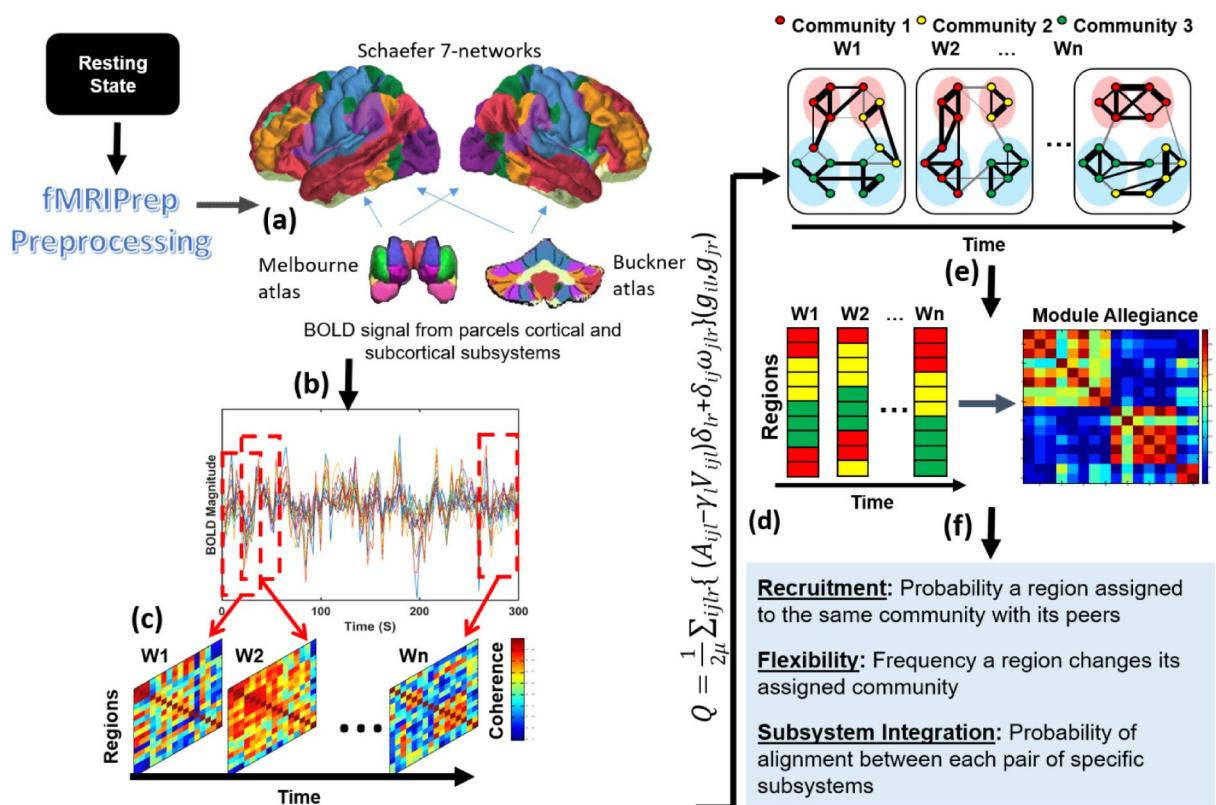

Fig. 1. Schematic overview of the approach. (**a**) BOLD signal was extracted from the Schaefer parcels corresponding to the Yeo 7-networks[53] (visual [purple], somatomotor [blue], DAN [green], VAN [violet], limbic [yellow], control [orange] and DMN [red]); thalamus [red], striatum (globus pallidus [not visible], nucleus accumbens [purple], caudate [violet] and putamen [green]) and mesial temporal (hippocampus [yellow] and amygdala [pink]) systems from Melbourne atlas[47] and 7 cerebellar subsystems (color coded based on its maximal functional correlation with a Schaefer cerebral network) using the Buckner atlas—at individual level[48]. (**b**) Time series were extracted from the Schaefer 200 parcels, Melbourne 54 parcels and 7 cerebellar parcels using RS fMRI data. (**c**) A sliding window strategy (length/step = 40/20 s, 23 windows in total) was used to generate inter-regional coherence matrices over time. (**d**) Dynamic community structure was detected by maximizing a multilayer modularity quality function[78]. (**e**) Community identities were sorted for each parcel over time (Module Allegiance[50,55]). (**f**) Dynamic properties were estimated[50,51,78]. DAN = dorsal attention network; VAN = ventral attention network; DMN = default mode network; RS fMRI = resting state functional MRI.

in multiple subcortical systems and multiple subcortico–cortico systems, with the added prediction that the observed abnormalities in these subcortico–cortico interactions would be correlated only in the FBTCS+ group.

Results

Demographical and clinical comparisons

The experimental groups (TLE, HP) did not differ in age, sex, IQ, or handedness[52] (see Table 1). The groups, however, did differ in the years of education attained, with HPs higher (Table 1). Accordingly, education was regressed out from the network properties with a linear regression model, and the residuals were taken for subsequent statistical analyses and inference (rmMANOVAs, RFs).

Subcortical and cortical dFC measures showing LTLE/HP group differences

The results revealed no significant difference between HPs and the LTLE group in recruitment and flexibility for any of the subcortical/cortical rmMANOVAs (see Table 2 and associated results in Supplement Section—Results 1). Thus, the findings that emerged reflected normative effects. For instance, recruitment showed hemisphere X subsystem effects for the thalamic/cortical and striatum/cortical models. Univariate, pairwise comparisons indicated the Visual, Somatomotor, and the VAN consistently showed greater recruitment in the left compared to right hemisphere. The DMN, on the other hand, showed greater recruitment in the right hemisphere. With regard to the subcortical systems, the anterior thalamus displayed greater recruitment in the right hemisphere

| | Left TLE group (55) | | | | | |
	FBTCS− (15)	FBTCS+ Remote (13)	FBTCS+ Current (27)	Healthy Participants (56)	F/χ^2	P
Age	42.08 ± 15.27	37.34 ± 10.87	40.01 ± 10.99	36.39 ± 9.96	1.360	0.259
Gender (male/female)	7/8	7/6	14/13	37/19	2.796	0.424
Education	14.87 ± 2.32	14.69 ± 2.21	14.48 ± 2.33	16.25 ± 2.89	**3.574**	**ª0.016**
ᵇIQ	96.14 ± 15.48	100.75 ± 19.17	96.77 ± 14.02	NA	0.718	0.492
Edinburgh Handedness, R/L/A	11/4/0	11/2/0	24/3/0	52/4/0	4.554	0.208
Age of seizure onset	25.21 ± 19.73	20.54 ± 11.38	28.37 ± 11.06	NA	1.411	0.253
Illness duration	18.20 ± 19.78	16.29 ± 15.39	11.56 ± 10.34	NA	1.113	0.337
Temporal pathology (NB/MTS/TT/O)	3/7/0/5	2/6/0/5	9/9/1/8	NA		
Seizure type						
FAS	2	0	0	NA		
FIAS	5	0	0	NA		
FIAS/FAS	8	0	0	NA		
FIAS+ FBTCS	0	6	15	NA		
FAS+ FBTCS	0	2	2	NA		
FIAS/FAS+ FBTCS	0	5	10	NA		
Current anti-epileptic drugs						
VGNC	6	11	17	NA		
GABA$_a$ agonist	0	1	2	NA		
SV2$_a$ receptor mediated	5	4	5	NA		
CRMP2 receptor mediated	5	3	11	NA		
Multi-action	2	0	3	NA		
VGCC	3	2	2	NA		

Table 1. Sample demographic and clinical characteristics. Continuous variables are presented as mean ± standard deviation; Temporal pathology was diagnosed by neuroradiologists specializing in epilepsy based upon presurgical MRI scans: NB = normal brain; MTS = mesial temporal sclerosis; TT = temporal tumour; O = Other MR signal abnormality (e.g., encephalomalacia, cavernoma). Left TLE groups: FBTCS− = focal seizures only; FBTCS+ = patients with a history of focal to bilateral tonic–clonic seizures. Seizure type: FAS = focal aware seizure; FIAS = focal imapaired aware seizures; FBTCS = focal to bilateral tonic–clonic seizures. Anti-epileptic drugs: VGNC = voltage-gated Na+ channel blockage, e.g. phenytoin, carbamazepine, oxcarbazepine, lamotrigine, rufinamide, eslicarbazepine, zonisamide (plus T Type Ca2+ channel blockage); GABAa agonist, e.g. diazepam, clonazepam, clobazam, lorazepam, traxene, phenobarbital; SV2a receptor mediated, e.g. levetiracetam; CRMP2 receptor mediated, e.g. lacosamide (plus VGNC blockage); Multi-action: e.g. Na+ valproate (VGNC+ GABAa agonist), topiramate (VGNC+ GABAa agonist+ AMPA/ kainate receptor blockage+ carbonic anhydrase inhibitor); VGCC = voltage-gated Ca++ channel blockage, e.g. pregabalin, gabapentin. Multiple anti-epileptic drugs from the same category for one patient were counted only once. For continuous variables, one-way ANOVAs were conducted. For categorical variables, χ^2 tests were carried out. Significant differences are highlighted in bold. ªPost Hoc Tests revealed a significant difference between FBTCS+ current and Healthy Participants (p = 0.029). ᵇDerived from general intellectual ability score of Weschler adult intelligence scale—IV.

Source	df or Hypothesis df/error df	F	Sig	Partial Eta Squared	Observed power	Source	df or hypothesis df/error df	F	Sig	Partial eta Squared	Observed power
Recruitment						**Flexibility**					
Among thalamus and cortical subsystems											
WS Hemisphere	1	2.028	0.157	0.018	0.292	[b]WS Hemisphere	**1**	**4.461**	**0.037**	**0.039**	**0.553**
WS Hemisphere X Group	1	0.485	0.488	0.004	0.106	WS Hemisphere X Group	1	0.407	0.525	0.004	0.097
WS Subsystems X Group	5.411	0.460	0.820	0.004	0.181	WS Subsystems X Group	5.404	0.673	0.666	0.006	0.255
[a]WS Hemisphere X Subsystem	**4.857**	**4.843**	**0.000**	**0.043**	**0.978**	[c]WS Hemisphere X Subsystem	**7.080**	**2.505**	**0.015**	**0.022**	**0.885**
WS Hemisphere X Subsystem X Group	4.857	0.516	0.759	0.005	0.190	WS Hemisphere X Subsystem X Group	7.080	0.585	0.770	0.005	0.257
BTWS Group	1/109	1.368	0.245	0.012	0.213	BTWS Group	1/109	1.192	0.277	0.011	0.191
Among striatum and cortical subsystems											
[d]WS Hemisphere	**1**	**4.170**	**0.044**	**0.037**	**0.526**	WS Hemisphere	1	0.118	0.732	0.001	0.063
WS Hemisphere X Group	1	2.418	0.123	0.022	0.338	WS Hemisphere X Group	1	0.281	0.597	0.003	0.082
WS Subsystems X Group	6.950	1.093	0.366	0.010	0.474	WS Subsystems X Group	7.749	0.357	0.939	0.003	0.171
[e]WS Hemisphere X Subsystem	**5.009**	**2.317**	**0.042**	**0.021**	**0.747**	[f]*WS Hemisphere X Subsystem*	*8.212*	*1.896*	*0.056*	*0.017*	*0.809*
WS Hemisphere X Subsystem X Group	5.009	1.540	0.176	0.014	0.541	WS Hemisphere X Subsystem X Group	8.212	0.647	0.742	0.006	0.309
BTWS Group	1/109	1.307	0.255	0.012	0.205	BTWS Group	1/109	0.194	0.660	0.002	0.072
Among mesial temporal and cortical subsystems											
[g]WS Hemisphere	**1**	**4.818**	**0.030**	**0.042**	**0.585**	WS Hemisphere	1	0.448	0.505	0.004	0.102
WS Hemisphere X Group	1	0.309	0.579	0.003	0.085	WS Hemisphere X Group	1	0.7.9	0.402	0.006	0.133
WS Subsystems X Group	4.895	0.853	0.510	0.008	0.304	WS Subsystems X Group	5.724	0.606	0.718	0.006	0.238
WS Hemisphere X Subsystem	3.744	1.941	0.107	0.017	0.564	WS Hemisphere X Subsystem	6.347	1.530	0.161	0.014	0.613
WS Hemisphere X Subsystem X Group	3.744	0.829	0.501	0.008	0.256	WS Hemisphere X Subsystem X Group	6.347	1.055	0.389	0.010	0.435
BTWS Group	1/109	2.082	0.152	0.019	0.299	BTWS Group	1/109	0.065	0.799	0.001	0.057
Among cerebellar/cortical subsystems											
WS Hemisphere						WS Hemisphere	1	0.032	0.858	0.000	0.054
WS Hemisphere X Group						WS Hemisphere X Group	1	1.134	0.289	0.010	0.184
WS Subsystems X Group			No recruitment for Cerebellar subsystems			WS Subsystems X Group	7.903	1.120	0.347	0.010	0.523
WS Hemisphere X Subsystem						[h]WS Hemisphere X Subsystem	**7.957**	**2.003**	**0.044**	**0.018**	**0.824**
WS Hemisphere X Subsystem X Group						[i]WS Hemisphere X Subsystem X Group	**7.957**	**2.142**	**0.030**	**0.019**	**0.854**
BTWS Group						BTWS Group	1/109	0.006	0.938	0.000	0.051

Table 2. Results of Healthy Participants versus LTLE group for two-way repeated-measures MANOVA for recruitment and flexibility within subcortical and cortical subsystems for the four subcortical/cortical subsystem combinations(thalamus, striatum, mesial-temporal and cerebellar subsystems with all cortical subsystems). The univariate test results showing main effects and interactions of condition, experimental group, and subsystems for recruitment and flexibility. Pairwise comparisons were also tested for the results showing a significant univariate effect to determine the nature of the differences between those variables (See suppl. section). WS—Within-subject effect, BTWS—Between-subject effect. Significant effects are highlighted in bold. *Multivariate effect is significant at p < 0.05 or less.

(thalamus/cortical model), while the caudate (striatum/cortical model) and posterior hippocampus (mesial temporal/cortical model, statistical trend p = 0.076) displayed greater recruitment in left hemisphere.

The rmMANOVA on flexibility also revealed significant hemisphere X subsystem interactions, reflecting normative dFC effects (n.b., thalamus/cortical, striatum/cortical, cerebellar/cortical models). Univariate pairwise comparisons showed greater flexibility in the left than right hemisphere for the Limbic (thalamus/cortical, striatum/cortical, cerebellar/cortical models) and DAN cortical subsystems (thalamus/cortical model). The somatomotor subsystem showed higher flexibility in the right hemisphere in the cerebellar/cortical model.

The rmMANOVA results for integration are shown in Table 3 (see associated results in Supplement Section—Results 2). The posterior thalamus/cortical model resulted in a hemisphere X subsystem X group interaction that approached statistical significance (multivariate p = 0.067; univariate p = 0.096), revealing increased left posterior thalamus/right Visual system integration in LTLE compared to HPs. Significant hemisphere X subsystem effects emerged in both the anterior and posterior thalamus/cortical models, involving greater intra- than cross-hemispheric connections as given by univariate comparisons (Table 3).

Source	df or Hypothesis df/error df	F	Sig	Partial Eta Squared	Observed Power
Between anterior thalamus/cortical subsystems					
WS Hemisphere	1	0.019	0.889	0.000	0.052
WS Hemisphere X Group	1	3.526	0.063	0.031	0.461
WS Subsystems X Group	4.562	1.102	0.357	0.010	0.374
[j]WS Hemisphere X Subsystem	**6.793**	**5.213**	**0.000**	**0.046**	**0.999**
WS Hemisphere X Subsystem X Group	6.793	0.339	0.932	0.003	0.154
BTWS Group	1/109	0.340	0.561	0.003	0.089
Between posterior thalamus/cortical subsystems					
WS Hemisphere	1	1.501	0.223	0.014	0.229
WS Hemisphere X Group	1	0.055	0.815	0.001	0.056
WS Subsystems X Group	6.051	0.747	0.613	0.007	0.300
[k]WS Hemisphere X Subsystem	**6.510**	**3.774**	**0.001**	**0.033**	**0.973**
[l]WS Hemisphere X Subsystem X Group	*6.510*	*1.773*	*0.096*	*0.016*	*0.698*
BTWS Group	1/109	0.686	0.409	0.006	0.130
Between Putamen/cortical subsystems					
WS Hemisphere	1	0.129	0.720	0.129	0.065
WS Hemisphere X Group	1	2.609	0.109	0.023	0.360
[m]WS Subsystems X Group	*4.625*	*2.144*	*0.064*	*0.019*	*0.682*
[n]WS Hemisphere X Subsystem	**6.398**	**7.149**	**0.000**	**0.062**	**1.000**
WS Hemisphere X Subsystem X Group	6.398	0.230	0.972	0.002	0.114
BTWS Group	1/109	0.201	0.655	0.002	0.073
Between Caudate/cortical subsystems					
WS Hemisphere	1	3.330	0.071	0.030	0.440
WS Hemisphere X Group	1	0.097	0.757	0.001	0.061
WS Subsystems X Group	4.261	0.801	0.532	0.007	0.266
[o]WS Hemisphere X Subsystem	**6.511**	**2.894**	**0.007**	**0.026**	**0.914**
WS Hemisphere X Subsystem X Group	6.511	0.688	0.672	0.006	0.288
BTWS Group	1/109	0.046	0.831	0.000	0.055
Between Globus Pallidus/cortical subsystems					
WS Hemisphere	1	2.295	0.133	0.021	0.324
WS Hemisphere X Group	1	0.928	0.338	0.008	0.159
WS Subsystems X Group	4.812	1.386	0.230	0.013	0.481
WS Hemisphere X Subsystem	7.194	0.891	0.515	0.008	0.396
WS Hemisphere X Subsystem X Group	7.194	0.945	0.473	0.009	0.419
BTWS Group	1/109	0.501	0.480	0.005	0.108
Between Nucleus Accumbens/cortical subsystems					
WS Hemisphere	1	0.558	0.457	0.005	0.115
WS Hemisphere X Group	1	0.067	0.796	0.001	0.058
WS Subsystems X Group	5.064	0.897	0.484	0.008	0.325
WS Hemisphere X Subsystem	*5.997*	*1.811*	*0.094*	*0.016*	*0.682*
WS Hemisphere X Subsystem X Group	5.997	0.546	0.773	0.005	0.221
BTWS Group	1/109	0.136	0.713	0.001	0.136
Between Anterior hippocampus/cortical subsystems					
WS Hemisphere	1	0.258	0.612	0.002	0.080
WS Hemisphere X Group	1	0.159	0.691	0.001	0.068
WS Subsystems X Group	5.400	0.994	0.424	0.009	0.373
[p]WS Hemisphere X Subsystem	**6.050**	**4.491**	**0.000**	**0.040**	**0.987**
WS Hemisphere X Subsystem X Group	6.050	1.047	0.394	0.010	0.419
BTWS Group	1/109	0.023	0.879	0.000	0.053
Between posterior hippocampus/cortical subsystems					
WS Hemisphere	1	0.580	0.448	0.005	0.117
WS Hemisphere X Group	1	0.527	0.469	0.005	0.111
WS Subsystems X Group	5.544	0.727	0.617	0.007	0.279
[q]WS Hemisphere X Subsystem	**6.333**	**5.359**	**0.00**	**0.047**	**0.997**
[r]WS Hemisphere X Subsystem X Group	**6.333**	**2.640**	**0.014**	**0.024**	**0.876**
BTWS Group	1/109	0.073	0.788	0.001	0.058
Continued					

Source	df or Hypothesis df/error df	F	Sig	Partial Eta Squared	Observed Power
Between amygdala/cortical subsystems					
WS Hemisphere	1	2.274	0.134	0.020	0.321
WS Hemisphere X Group	1	0.001	0.977	0.000	0.050
WS Subsystems X Group	4.964	0.384	0.859	0.004	0.150
[s]WS Hemisphere X Subsystem	**6.304**	**3.874**	**0.001**	**0.034**	**0.974**
WS Hemisphere X Subsystem X Group	6.304	1.296	0.254	0.012	0.527
BTWS Group					
Between Cereb1/cortical subsystems					
WS Hemisphere	1	2.011	0.159	0.018	0.290
WS Hemisphere X Group	1	2.033	0.157	0.018	0.293
WS Subsystems X Group	5.160	0.574	0.725	0.005	0.215
[t]WS Hemisphere X Subsystem	**5.740**	**2.009**	**0.066**	**0.018**	**0.721**
[u]*WS Hemisphere X Subsystem X Group*	*5.740*	*1.528*	*0.170*	*0.014*	*0.580*
BTWS Group	1/109	0.134	0.715	0.001	0.065
Between Cereb2/cortical subsystems					
WS Hemisphere	1	0.110	0.740	0.001	0.063
[v]WS Hemisphere X Group	**1**	**6.068**	**0.015**	**0.053**	**0.685**
WS Subsystems X Group	5.407	0.799	0.560	0.007	0.301
[w]WS Hemisphere X Subsystem	**6.106**	**3.009**	**0.006**	**0.027**	**0.912**
WS Hemisphere X Subsystem X Group	6.106	0.806	0.567	0.007	0.325
BTWS Group	1/109	0.905	0.343	0.008	0.156
Between Cereb3/cortical subsystems					
WS Hemisphere	1	0.055	0.814	0.001	0.056
WS Hemisphere X Group	1	0.459	0.500	0.004	0.103
WS Subsystems X Group	5.728	1.561	0.160	0.014	0.590
[x]WS Hemisphere X Subsystem	**6.467**	**2.185**	**0.038**	**0.020**	**0.801**
WS Hemisphere X Subsystem X Group	6.467	0.743	0.625	0.007	0.310
BTWS Group	1/109	0.434	0.512	0.004	0.100
Between Cereb4/cortical subsystems					
WS Hemisphere	1	0.791	0.376	0.007	0.143
WS Hemisphere X Group	1	0.013	0.910	0.000	0.051
WS Subsystems X Group	5.309	1.740	0.119	0.016	0.621
[y]WS Hemisphere X Subsystem	**6.169**	**4.574**	**0.000**	**0.040**	**0.989**
WS Hemisphere X Subsystem X Group	6.169	0.383	0.895	0.003	0.164
BTWS Group	1/109	0.038	0.847	0.000	0.054
Between Cereb5/cortical subsystems					
WS Hemisphere	1	0.014	0.906	0.000	0.052
WS Hemisphere X Group	1	0.047	0.829	0.000	0.055
WS Subsystems X Group	5.707	0.486	0.810	0.004	0.194
WS Hemisphere X Subsystem	6.788	1.585	0.139	0.014	0.654
WS Hemisphere X Subsystem X Group	6.788	1.732	0.101	0.016	0.701
BTWS Group	1/109	0.433	0.512	0.004	0.100
Between Cereb6/cortical subsystems					
WS Hemisphere	1	0.880	0.350	0.008	0.153
[z]WS Hemisphere X Group	**1**	**4.831**	**0.030**	**0.042**	**0.587**
WS Subsystems X Group	5.179	1.617	0.151	0.015	0.576
[aa]WS Hemisphere X Subsystem	**6.395**	**2.719**	**0.011**	**0.024**	**0.889**
WS Hemisphere X Subsystem X Group	6.395	0.468	0.843	0.004	0.198
BTWS Group	1/109	0.217	0.643	0.002	0.075
Between Cereb7/cortical subsystems					
WS Hemisphere	1	1.474	0.227	0.013	0.225
Continued					

Source	df or Hypothesis df/error df	F	Sig	Partial Eta Squared	Observed Power
WS Hemisphere X Group	1	1.907	0.170	0.017	0.278
WS Subsystems X Group	4.915	1.257	0.281	0.011	0.444
[ab]WS Hemisphere X Subsystem	**7.208**	**3.540**	**0.001**	**0.031**	**0.975**
WS Hemisphere X Subsystem X Group	7.208	0.250	0.974	0.002	0.126
BTWS Group	1/109	0.035	0.852	0.000	0.054

Table 3. Results of Healthy Participants versus LTLE group for two-way repeated-measures MANOVA for subsystem integration between the four subcortical/cortical subsystem combinations (thalamus, striatum, mesial-temporal and cerebellar subsystems with all cortical subsystems). The univariate test results showing main effects and interactions of condition, experimental group, and subsystems for integration. Pairwise comparisons were also tested for the results showing a significant univariate effect to determine the nature of the differences between those variables (See suppl. section). WS—Within-subject effect, BTWS—Between-subject effect. *Multivariate effect is significant at p < .05 or less. Significant differences are highlighted in bold. Trends are italicized.

In the four striatum/cortical models, the subsystem X group effect approached significance (univariate p = 0.064; Table 3), revealing reduced putamen/Limbic integration in LTLE compared to HPs. Significant hemisphere X subsystem effects emerged in the striatum/cortical models (for putamen and caudate), involving greater intra- than cross-hemispheric connections as given by univariate comparisons (these effects are listed in Table 3).

Among the three mesial-temporal models, a significant hemisphere X subsystem X group (univariate p = 0.014) interaction was observed for the posterior hippocampus/cortical model. Compared to HPs, TLE showed higher cross-hemispheric integrations involving left posterior hippocampus/right Visual (univariate p = 0.03) and right posterior hippocampus/left VAN (univariate p = 0.066) subsystems. In contrast, there was reduced right posterior hippocampus/right Control system intra-hemispheric integration (univariate p = 0.046) in the LTLE group. This model also showed significant hemisphere X subsystem effects with greater intra- than cross-hemispheric connections as given by univariate comparisons (these effects are listed in Table 2).

In the cerebellum-based models, a hemisphere X subsystem X group effect approached statistical significance (multivariate p = 0.075) for right cereb-1/cortical integration, involving reduced right cereb1/left Visual integration in the LTLE group compared to HPs (pairwise comparison, p = 0.029, univariate effect non-significant, see Table 3). A significant hemisphere X group effect for cereb-2/cortical (multivariate, p = 0.015) and cereb-6/cortical (multivariate, p = 0.03) integrations was present. The pattern of integrations indicated that the LTLE group had a higher right cereb2/cortical integrations compared to those of left cereb2 (F(1,109) = 3.873, p = 0.052), whereas the HPs had a higher right cereb6/cortical integrations compared to those of left cereb6 (F(1,109) = 4.962, p = 0.028). Compared to the other subcortical subsystems, the normative hemisphere X subsystem effects for cerebellar subsystems were primarily preferential towards inter-hemispheric integrations, with these integrations higher than the intra-hemispheric integrations for cereb1, cereb2, cereb3 and cereb4. For cereb6 and cereb7 there was no clear intra/inter hemispheric preference for cortical integrations. See Table 3 for a complete list of integrations involved in this effect.

Subcortical and cortical dFC measures showing FBTCS+ /FBTCS− or FBTCS+ current/remote group differences

The rmMANOVA on the dFC deviation measures revealed several group differences (Tables 4, 5; Fig. 2; and associated results in Supplement Section—Results 3 & 4). With regard to recruitment, there were two significant subsystem X group effects involving the thalamus/cortical model. There was increased recruitment in DAN in the FBTCS+ current group compared to FBTCS− (univariate p = 0.034), with FBTCS+ current also showing increased recruitment in the anterior thalamus compared to both FBTCS+ remote (univariate p = 0.013) and the FBTCS− groups (univariate p = 0.002). The FBTCS+ remote group also showed increased recruitment in DAN (univariate p = 0.005) compared to the FBTCS− group. Both the FBTCS+ remote (univariate p = 0.008) and FBTCS+ current (univariate p = 0.021) groups showed greater recruitment in the DAN compared to the FBTCS− group (striatum/cortical model). The FBTCS+ current group also showed increased recruitment in the Limbic network (univariate p = 0.029) compared to the FBTCS+ remote group (striatum/cortical model).

The rmMANOVAs on flexibility produced a very limited number of effects. In the thalamus/cortical model there was a hemisphere X group effect (multivariate p = 0.028), indicating higher flexibility in the FBTCS+ current (univariate p = 0.044) group in the left compared to the right hemisphere. A normative hemisphere X subsystem effect was observed in TLE as a whole, involving increased flexibility in the DMN (right > left hemisphere, p = 0.001), anterior hippocampus (right > left hemisphere, p = 0.054), and amygdala (right > left, p = 0.035); all involving the mesial temporal/cortical model. In addition, increased flexibility in the DMN (= p.007), Cereb4 (p = 0.009), and Cereb7 (p = 0.024), all right greater than left hemisphere, were present involving the cerebellar/cortical model.

With regard to integration, there were few significant group effects. In the posterior thalamus/cortical model there were significant hemisphere X subsystem effects with cross hemispheric posterior thalamic/cortical pairs showing higher integration than the pairs in the same hemisphere (see Table 5). Group differences were observed in the striatum/cortical model, involving a subsystem X group effect, reflecting increased integration

Source	df or hypothesis df/error df	F	Sig	Partial eta squared	Observed power	Source	df or hypothesis df/error df	F	Sig	Partial eta squared	Observed power
Recruitment						**Flexibility**					
Among thalamus and cortical subsystems											
WS Hemisphere	1	0.445	0.508	0.008	0.100	WS Hemisphere	1	0.666	0.418	0.013	0.126
WS Hemisphere X Group	2	0.223	0.801	0.009	0.083	[b]WS Hemisphere X Group	**2**	**3.820**	**0.028**	**0.128**	**0.669**
[a]WS Subsystems X Group	**14.299**	**2.476**	**0.002**	**0.087**	**0.986**	WS Subsystems X Group	11.243	1.227	0.267	0.045	0.673
WS Hemisphere X Subsystem	6.544	0.607	0.739	0.012	0.253	WS Hemisphere X Subsystem	5.903	1.463	0.191	0.027	0.562
WS Hemisphere X Subsystem X Group	13.088	0.874	0.582	0.033	0.539	WS Hemisphere X Subsystem X Group	11.806	1.119	0.344	0.041	0.639
BTWS Group	2/52	1.574	0.217	0.057	0.319 + 84	BTWS Group	2/52	0.107	0.899	0.004	0.066
Among striatum and cortical subsystems											
WS Hemisphere	1	2.997	0.089	0.054	0.397	WS Hemisphere	1	1.173	0.284	0.022	0.186
WS Hemisphere X Group	2	0.724	0.490	0.027	0.166	WS Hemisphere X Group	2	0.480	0.622	0.018	0.124
[c]WS Subsystems X Group	**17.359**	**2.098**	**0.006**	**0.075**	**0.983**	WS Subsystems X Group	13.437	0.729	0.739	0.027	0.456
WS Hemisphere X Subsystem	9.221	1.622	0.104	0.030	0.764	WS Hemisphere X Subsystem	5.751	1.092	0.367	0.021	0.420
WS Hemisphere X Subsystem X Group	18.442	0.576	0.266	0.044	0.822	WS Hemisphere X Subsystem X Group	11.502	0.866	0.579	0.032	0.495
BTWS Group	2/52	0.933	0.400	0.035	0.203	BTWS Group	2/52	0.243	0.785	0.009	0.086
Among mesial temporal and cortical subsystems											
WS Hemisphere	1	2.336	0.133	0.043	0.323	WS Hemisphere	1	1.997	0.164	0.037	0.284
WS Hemisphere X Group	2	0.124	0.884	0.005	0.068	WS Hemisphere X Group	2	0.275	0.760	0.010	0.091
WS Subsystems X Group	7.984	0.953	0.474	0.035	0.438	WS Subsystems X Group	9.424	0.449	0.913	0.017	0.225
WS Hemisphere X Subsystem	3.665	1.182	0.320	0.022	0.350	[d]WS Hemisphere X Subsystem	**4.795**	**2.990**	**0.013**	**0.054**	**0.845**
WS Hemisphere X Subsystem X Group	7.329	0.759	0.628	0.028	0.331	[e]*WS Hemisphere X Subsystem X Group*	*9.590*	*1.677*	*0.090*	*0.061*	*0.785*
BTWS Group	2/52	2.158	0.126	0.077	0.422	BTWS Group	2/52	0.803	0.454	0.030	0.180
Among cerebellar/cortical subsystems											
WS Hemisphere						WS Hemisphere	1	2.207	0.143	0.041	0.308
WS Hemisphere X Group						WS Hemisphere X Group	2	0.203	0.817	0.008	0.080
WS Subsystems X Group	No recruitment for cerebellar systems					WS Subsystems X Group	15.173	1.012	0.442	0.037	0.669
WS Hemisphere X Subsystem						[f]WS Hemisphere X Subsystem	**7.362**	**2.674**	**0.009**	**0.049**	**0.913**
WS Hemisphere X Subsystem X Group						WS Hemisphere X Subsystem X Group	14.723	1.216	0.257	0.045	0.761
BTWS Group						BTWS Group	2/52	0.440	0.646	0.017	0.118

Table 4. Results of FBTCS− versus FBTCS+ remote and FBTCS+ current group for two-way repeated-measures MANOVA for the Z scores of recruitment and flexibility within subcortical and cortical subsystems for the four subcortical/cortical subsystem combinations (thalamus, striatum, mesial-temporal and cerebellar subsystems with all cortical subsystems). The univariate test results showing main effects and interactions of condition, experimental group, and subsystems for recruitment and flexibility. Pairwise comparisons were also tested for the results showing a significant univariate effect to determine the nature of the differences between those variables (See suppl. section). WS—Within-subject effect, BTWS—Between-subject effect. *Multivariate effect is significant at p < 0.05 or less. Significant effects are highlighted in bold.

in the FBTCS+ current compared to the FBTCS− group between the caudate/left VAN (univariate, p = 0.007) and caudate/right VAN (univariate, p = 0.07). The current compared to the remote FBTCS+ group also showed a greater integration between caudate/left Control (univariate, p = 0.009). There was also a significant hemisphere X group effect (multivariate, p = 0.021). Post hoc univariate testing revealed that within the FBTCS+ group, the hemispheres differed (p = 0.009), with the right compared to left caudate showing higher integrations with the cortical systems. With regard to the mesial-temporal subsystems, all three displayed significantly higher cross-compared to within-hemispheric integrations (Table 5). These hemisphere X subsystem effects are listed in Table 5. With regard to the cerebellar/cortical subsystems, only cereb5 showed a significant multivariate group effect (subsystem X group, p = 0.009), involving increased cereb5 integration with the left (univariate, p = 0.031) and right (univariate, p = 0.014) VAN in the FBTCS+ current compared to the FBTCS− group. Compared to the FBTCS− group, FBTCS+ remote showed increased integration between cereb5/right VAN (univariate, p = 0.014). Also, the FBTCS+ current group showed increased cereb-5/left DMN integration compared to FBTCS+ remote.

Source	df or Hypothesis df/error df	F	Sig	Partial Eta Squared	Observed Power
Between anterior thalamus/cortical subsystems					
[g]**WS Hemisphere**	**1**	**6.260**	**0.016**	**0.107**	**0.690**
WS Hemisphere X Group	2	0.833	0.440	0.031	0.185
WS Subsystems X Group	9.893	0.841	0.588	0.031	0.439
WS Hemisphere X Subsystem	6.656	0.880	0.518	0.017	0.370
WS Hemisphere X Subsystem X Group	13.312	0.675	0.791	0.025	0.419
BTWS Group	2/52	0.064	0.939	0.002	0.059
Between posterior thalamus/cortical subsystems					
WS Hemisphere	1	0.048	0.827	0.001	0.055
WS Hemisphere X Group	2	0.146	0.864	0.006	0.071
WS Subsystems X Group	12.874	0.608	0.846	0.023	0.367
[h]**WS Hemisphere X Subsystem**	**5.630**	**2.893**	**0.011**	**0.053**	**0.876**
WS Hemisphere X Subsystem X Group	11.259	0.922	0.521	0.034	0.520
BTWS Group	2/52	0.153	0.859	0.006	0.072
Between Putamen/cortical subsystems					
[i]*WS Hemisphere*	*1*	*3.357*	*0.073*	*0.061*	*0.436*
WS Hemisphere X Group	2	0.145	0.865	0.006	0.071
WS Subsystems X Group	9.415	1.132	0.340	0.042	0.570
WS Hemisphere X Subsystem	5.881	1.134	0.342	0.021	0.442
WS Hemisphere X Subsystem X Group	11.762	0.971	0.476	0.036	0.561
BTWS Group	2/52	0.091	0.914	0.003	0.063
Between Caudate/cortical subsystems					
WS Hemisphere	1	0.652	0.423	0.012	0.125
[j]**WS Hemisphere X Group**	**2**	**4.173**	**0.021**	**0.138**	**0.710**
[k]**WS Subsystems X Group**	**9.067**	**1.935**	**0.048**	**0.069**	**0.836**
WS Hemisphere X Subsystem	6.487	1.331	0.239	0.025	0.544
WS Hemisphere X Subsystem X Group	12.974	0.545	0.895	0.021	0.328
BTWS Group	2/52	0.418	0.661	0.016	0.114
Between Globus Pallidus/cortical subsystems					
WS Hemisphere	1	1.318	0.256	0.025	0.203
WS Hemisphere X Group	2	0.052	0.950	0.002	0.057
WS Subsystems X Group	10.382	0.623	0.799	0.023	0.331
WS Hemisphere X Subsystem	6.257	1.297	0.256	0.024	0.520
WS Hemisphere X Subsystem X Group	12.515	0.642	0.812	0.024	0.382
BTWS Group	2/52	0.060	0.942	0.002	0.059
Between Nucleus Accumbens/cortical subsystems					
WS Hemisphere	1	0.252	0.618	0.005	0.078
WS Hemisphere X Group	2	0.243	0.786	0.009	0.086
WS Subsystems X Group	11.389	0.412	0.954	0.016	0.229
WS Hemisphere X Subsystem	6.738	1.566	0.147	0.029	0.640
WS Hemisphere X Subsystem X Group	13.476	0.883	0.574	0.033	0.554
BTWS Group	2/52	0.084	0.920	0.003	0.062
Between Anterior hippocampus/cortical subsystems					
WS Hemisphere	1	0.922	0.341	0.017	0.156
WS Hemisphere X Group	2	0.474	0.625	0.018	0.123
WS Subsystems X Group	9.124	0.675	0.733	0.025	0.334
[l]*WS Hemisphere X Subsystem*	*5.670*	*1.881*	*0.088*	*0.035*	*0.677*
WS Hemisphere X Subsystem X Group	11.341	0.661	0.780	0.025	0.371
BTWS Group	2/52	0.213	0.809	0.008	0.082
Between Posterior hippocampus/cortical subsystems					
WS Hemisphere	1	0.021	0.887	0.000	0.052
WS Hemisphere X Group	2	1.076	0.348	0.040	0.229
WS Subsystems X Group	10.473	0.734	0.699	0.027	0.395
[m]**WS Hemisphere X Subsystem**	**6.076**	**5.113**	**0.000**	**0.090**	**0.994**
WS Hemisphere X Subsystem X Group	12.152	1.284	0.226	0.047	0.725
BTWS Group	2/52	1.272	0.289	0.047	0.264
Continued					

Source	df or Hypothesis df/error df	F	Sig	Partial Eta Squared	Observed Power
Between Amygdala/cortical subsystems					
WS Hemisphere	1	0.003	0.956	0.000	0.050
WS Hemisphere X Group	2	0.072	0.931	0.003	0.060
WS Subsystems X Group	9.767	1.102	0.361	0.041	0.567
[n]*WS Hemisphere X Subsystem*	*5.507*	*1.866*	*0.093*	*0.035*	*0.663*
WS Hemisphere X Subsystem X Group	11.015	1.081	0.376	0.040	0.597
BTWS Group	2/52	0.638	0.532	0.024	0.151
Between Cereb1/cortical subsystems					
WS Hemisphere	1	2.112	0.152	0.039	0.297
WS Hemisphere X Group	2	0.004	0.996	0.000	0.051
WS Subsystems X Group	10.360	1.110	0.354	0.041	0.590
[o]**WS Hemisphere X Subsystem**	**5.765**	**2.274**	**0.039**	**0.042**	**0.778**
WS Hemisphere X Subsystem X Group	11.529	1.295	0.223	0.047	0.712
BTWS Group	2/52	0.201	0.818	0.008	0.080
Between Cereb2/cortical subsystems					
[p]**WS Hemisphere**	**1**	**7.349**	**0.009**	**0.124**	**0.758**
WS Hemisphere X Group	2	0.064	0.938	0.002	0.059
WS Subsystems X Group	11.076	0.946	0.497	0.035	0.528
WS Hemisphere X Subsystem	6.041	1.195	0.322	0.022	0.462
WS Hemisphere X Subsystem X Group	12.081	0.655	0.795	0.025	0.382
BTWS Group	2/52	0.447	0.642	0.017	0.119
Between Cereb3/cortical subsystems					
WS Hemisphere	1	2.312	0.134	0.043	0.320
WS Hemisphere X Group	2	0.066	0.936	0.003	0.059
WS Subsystems X Group	10.786	0.817	0.621	0.030	0.449
WS Hemisphere X Subsystem	5.982	0.919	0.481	0.017	0.363
WS Hemisphere X Subsystem X Group	11.964	0.785	0.665	0.029	0.459
BTWS Group	2/52	0.495	0.612	0.019	0.127
Between Cereb4/cortical subsystems					
WS Hemisphere	1	0.001	0.982	0.000	0.050
WS Hemisphere X Group	2	2.207	0.120	0.078	0.431
WS Subsystems X Group	10.856	0.786	0.653	0.029	0.433
WS Hemisphere X Subsystem	5.628	0.553	0.757	0.011	0.214
WS Hemisphere X Subsystem X Group	11.256	0.820	0.623	0.031	0.462
BTWS Group	1/109	0.598	0.553	0.022	0.144
Between Cereb5/cortical subsystems					
WS Hemisphere	1	0.051	0.822	0.001	0.056
WS Hemisphere X Group	2	0.390	0.679	0.015	0.110
[q]*WS Subsystems X Group*	*10.910*	*1.684*	*0.077*	*0.061*	*0.828*
[r]**WS Hemisphere X Subsystem**	**6.179**	**2.791**	**0.011**	**0.051**	**0.886**
WS Hemisphere X Subsystem X Group	12.357	0.516	0.908	0.019	0.301
BTWS Group	2/52	0.939	0.397	0.035	0.204
Between Cereb6/cortical subsystems					
[s]**WS Hemisphere**	**1**	**7.429**	**0.009**	**0.125**	**0.763**
WS Hemisphere X Group	2	0.886	0.418	0.033	0.195
WS Subsystems X Group	10.847	1.018	0.430	0.038	0.559
WS Hemisphere X Subsystem	6.290	0.903	0.496	0.017	0.367
WS Hemisphere X Subsystem X Group	12.579	0.592	0.856	0.022	0.352
BTWS Group	2/52	1.442	0.246	0.053	0.295
Between Cereb7/cortical subsystems					
[t]**WS Hemisphere**	**1**	**4.956**	**0.030**	**0.087**	**0.589**
Continued					

Source	df or Hypothesis df/error df	F	Sig	Partial Eta Squared	Observed Power
WS Hemisphere X Group	2	1.532	0.226	0.056	0.311
WS Subsystems X Group	10.148	1.015	0.431	0.038	0.537
WS Hemisphere X Subsystem	6.793	0.403	0.896	0.008	0.177
WS Hemisphere X Subsystem X Group	13.587	0.610	0.852	0.023	0.381
BTWS Group	2/52	0.764	0.471	0.029	0.173

Table 5. Results of two-way repeated-measures MANOVA (FBTCS− versus FBTCS+ remote versus FBTCS+ current) for the Z scores of subsystem integration between the four subcortical/cortical subsystem combinations (thalamus, striatum, mesial-temporal and cerebellar subsystems with all cortical subsystems). The univariate test results showing main effects and interactions of condition, experimental group, and subsystems for integration. Pairwise comparisons were also tested for the results showing a significant univariate effect to determine the nature of the differences between those variables (See suppl. section). WS—Within-subject effect, BTWS—Between-subject effect. *Multivariate effect is significant at p < 0.05 or less. Significant differences are highlighted in bold. Trends are italicized.
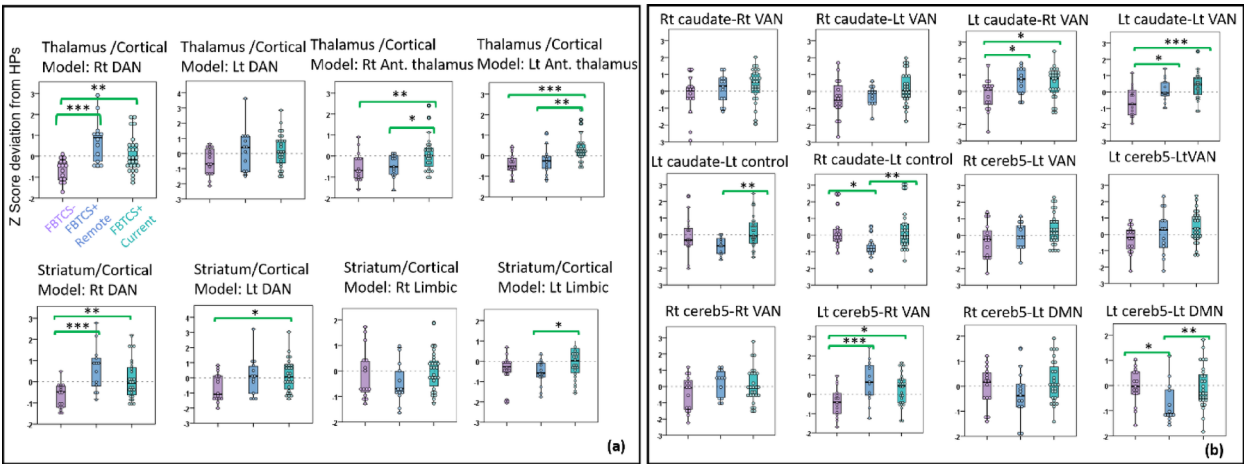
Fig. 2. Regional allegiance preference. Abnormality in recruitment (**a**) and subcortico–cortico integrations (**b**) in the 3 patient groups (FBTCS−, FBTCS+ remote, FBTCS+ current) based on rmMANOVA models (flexibility not shown) (X–Y axis identical throughout). Asterisk indicates pairwise group differences, ***P < 0.01, **P < 0.05, *P < 0.1 (all Bonferroni corrected). Error bars reflect standard error (SE). FBTCS− = focal seizure group; FBTCS+ = focal-to-bilateral tonic clonic seizures; rmMANOVA = repeated measures multivariate analysis of variance; DAN = dorsal attention network; Ant. = anterior; VAN = ventral attention network; DMN = default mode network.

Cereb-1 (multivariate, p = 0.024) and cereb-5 (multivariate, p < 0.0001) displayed significant hemisphere X subsystem effects, without any clear indications of a cross- or intra-hemispheric integration pattern as evident in other subcortical systems (see Table 5). See Table 5 for a complete list of integrations involved in this effect.

Random Forest models for selection (ranking) of dFC features distinguishing FBTCS+ / FBTCS− or FBTCS+ current/remote groups

The number of features emerging from rmMANOVA models from HP versus LTLE group comparisons was limited and were mostly trends. Therefore, a RF classification was not run for the LTLE/HP comparison.

Results of our two RF models are displayed in Table 6. The classification accuracy was strong for both RF models (FBTCS+ /FBTCS− model = 70.0% accuracy; FBTCS+ current/FBTCS+ remote = 78.18% accuracy). A full list of the features with variable importance (significance ratios) of 0.60 or greater is shown in Table 6. The FBTCS+ /FBTCS− RF model revealed that FBTCS+ status was associated with increased recruitment of right DAN (variable importance ratio, VIR = 1) and the left anterior thalamus (VIR = 0.94). FBTCS+ status was also associated with increased integration between the left caudate/left VAN (VIR = 1) and the right cereb5/left VAN (VIR = 1). The FBTCS+ current/remote RF model showed that current FBTCS+ status was associated with increased recruitment of left anterior thalamus (VIR = 0.966) and increased integration between the left caudate/left Control (VIR = 0.984), right caudate/left Control (VIR = 1), and left cereb5/left DMN (VIR = 1) subsystems.

Correlations among RF classifiers of FBTCS+ /FBTCS− and FBTCS+ current/remote status

Overall, the important dFC measures (see Table 6) showed few significant associations, suggesting a strong degree of independence among them. A positive correlation was obtained between recruitment of right DAN

Subcortical/cortical model	Dynamic FC metric	FBTCS+/FBTCS−	p value	Significance ratio
A. FBTCS+ versus FBTCS− Outcomes (Classification Accuracy = 70%)				
Thalamus/Cortical	Recruitment Right DAN	FBTCS+	0.001	1
Thalamus/Cortical	Recruitment Left anterior thalamus	FBTCS+	0.007	0.94
Striatum/Cortical	Recruitment Right DAN	FBTCS+	0.001	1.000
Striatum/Cortical	Integration Left caudate/Left VAN	FBTCS+	0.001	1.000
Cerebellum/Cortical	Integration Right cereb5/Left VAN	FBTCS+	0.060	1.000
Subcortical/cortical model	**Dynamic FC metric**	**FBTCS+remote/ current History**	**p value**	**Significance ratio**
B. FBTCS+Current versus FBTCS+Remote Outcomes (Classification Accuracy = 78.18%)				
Thalamus/Cortical	Recruitment Left Anterior thalamus	FBTCS+Current	0.008	0.966
Striatum/Cortical	Integration Left caudate/Left control	FBTCS+Current	0.005	0.984
Striatum/Cortical	Integration Right caudate/Left control	FBTCS+Current	0.008	1.000
Cerebellum/Cortical	Integration Left cereb5/Left DMN	FBTCS+Current	0.020	1.000

Table 6. Random forest model results.

(thalamus/cortical model) and recruitment of the right DAN in the striatum/cortical model in both FBTCS− (r = 0.915, p < 0.0001) and FBTCS+ (r = 0.971, p < 0.0001), with this association reliably higher in the FBTCS+ group (p = 0.048). Recruitment of left anterior thalamus was found to be positively correlated with the right cereb-5/left VAN integration in FBTCS− (r = 0.560, p = 0.030) but not the FBTCS+ group (r = 0.120, p = 0.459). Recruitment of the left anterior thalamus and integration between the left cereb-5/left DMN trended toward significance in FBTCS+ remote (r = 0.533, p = 0.061), but had no reliable relationship in the FBTCS+ current group.

Lastly, a positive correlation was observed between two integration features (left caudate/left Control with right caudate/left Control) in both the FBTCS+ remote (r = 0.517, p = 0.070) and FBTCS+ current (r = 0.591, p = 0.001) groups, but the group comparison revealed these correlations were not statistically different.

Correlations between clinical epilepsy variables and RF classifiers of FBTCS+ /FBTCS− and FBTCS+ current/remote Status

In our correlational analyses with the clinical epilepsy variables, we focused on the dFC metrics that proved to be reliable classifiers of group membership in our two RF models (see Table 6A, B). Age of seizure onset and illness duration showed no reliable relationship to recruitment in the right DAN or recruitment in the left anterior thalamus in either the FBTCS+ or FBTCS− group. Age of seizure onset or illness duration bore no reliable relationship to recruitment of the right DAN (striatum/cortical model). Similarly, age of seizure onset was not reliably associated with the left caudate/left VAN integration in either the FBTCS+ or FBTCS− group. An association between higher illness duration and higher left caudate/left VAN integration approached statistical significance (r = 0.278, p = 0.083) in FBTCS+ , but no such association was observed in the FBTCS− group. The association between older age of seizure onset and higher right cereb-5/left VAN integration approached significance in FBTCS+ (r = 0.310, p = 0.052), but not the FBTCS− (r = 0.410, p = 0.145) group. These correlations did not differ between the groups.

Regarding the FBTCS+ remote and current RF models (see Table 6B), the left anterior thalamus recruitment was not associated with age of seizure onset nor illness duration in either group. Higher integration between left caudate/left Control was associated with older age of seizure onset (r = 0.615, p = 0.025), and shorter illness duration (r = -0.656, p = 0.015) in the FBTCS+ remote group. No significant correlations with clinical epilepsy variables emerged in the FBTCS+ current group. Note, the right caudate/left Control RF feature (see Table 6B) was not associated with any of the clinical epilepsy variables in either the FBTCS+ remote or current groups. The left cereb-5/left DMN integration feature bore no reliable association with age of seizure onset, but longer illness duration was associated with higher left cereb-5/left DMN integration in the FBTCS+ current group (r = 0.425, p = 0.027).

Discussion

Pursuant to a network science perspective[42], we investigated the whole brain dynamic intrinsic functional connectivity within and between multiple subcortical (thalamus, striatum, mesial temporal, cerebellum), and cortical systems (seven canonical intrinsic functional systems[53]). We demonstrated that left TLE patients possessed a set of abnormal subcortical/cortical communication dynamics at rest, and showed that these abnormalities differ in the context of an FBTCS+ history. We also observed several normative subcortical-cortical dynamics (n.b., no group difference), providing insight into the intrinsic dynamics of the normal brain during the baseline, tonic state (see Tables 2 and 3).

Normative hemispheric biases in communication were evident within several subcortical systems (higher right than left anterior thalamic recruitment; higher left than right caudate and posterior hippocampus recruitment; see Table 2). These data provided the first report of normative intrinsic communication dynamics within each of

these subcortical systems, demonstrating that such dynamics are not balanced across the hemispheres. Cortical subsystems also showed a hemispheric bias in their within-system communication (e.g., Visual, Somatomotor, and VAN), displaying significantly higher levels of left compared to right hemisphere recruitment (Table 2). While hemispheric asymmetries in the dynamics of language networks have been reported by our lab[54] and others[55], normative asymmetries in these other networks have not been reported. Note, we checked to see if these asymmetries, particularly somatomotor, were associated with handedness (a surrogate for hemispheric dominance) in our sample, and this was not the case (See supplementary text). Regarding these normative findings, the DMN differed, showing consistently greater recruitment in the right compared left hemisphere. This hemispheric bias in the tonic, resting state status of the DMN has also not been reported previously. Normative hemispheric biases in our dFC measures of flexibility were also evident in several cortical networks (Limbic, DAN, Somatomotor) (Table 2). These data refer to communication outside a given network, revealing that several cortical systems operated with a hemispheric bias as they showed a propensity for left hemisphere intrinsic communication in the case of the Limbic and DAN, and more right hemisphere communication in the case of the somatomotor system. Lastly, our integration data demonstrated that intra- not cross-hemispheric subcortical/cortical communication was normative, with thalamus/cortical, mesial temporal/cortical, and striatum/cortical integrations all showing this pattern (n.b., cerebellar/cortical was the exception with six of seven cerebellum/cortical models showing prominent contralateral communication with cortex; see Table 3).

Before reporting on our RF classification models, it is worth noting that our use of deviation scores allowed us to identify several dFC abnormalities within LTLE and its subgroups. For instance, within LTLE subcortical/cortical communication (i.e., flexibility) was generally higher in the hemisphere contralateral to the seizures (e.g., mesial temporal/cortical [DMN, right > left; anterior hippocampus: right > left and amygdala: right > left] and cerebellar/cortical [DMN: right > left, Cereb4: right > left, Cereb7: right > left]) models (Table 4). The LTLE patients compared to HPs also showed several abnormally heightened cross-hemispheric integrations (left posterior thalamus and left posterior hippocampus with the right Visual network; right posterior hippocampus with left VAN; Table 5). Similarly, all the three mesial-temporal subsystems had more cross- than intra-hemispheric integrations with the cortical subsystems (Table 5). Cereb1 and cereb5 showed few hemisphere X subsystem effects without any clear trend towards a greater cross-hemispheric or ipsilateral integrations (Table 5). Interestingly, the hemisphere X subsystem effects within LTLE group were the opposite pattern of what was observed in the combined HP/LTLE sample as a whole (normatively).

These signs of greater cross-hemispheric subcortical/cortical integration indicated a deviation within LTLE from the normative pattern of ipsilateral subcortical/cortical functional connections described above in Sect. 4.1. There were also indications of abnormally reduced integrations for LTLE (striatum/putamen with left and right Limbic, right posterior hippocampus with right Control; see Table 3). These mesial-temporal and putamen-Limbic integration abnormalities are consistent with dysfunction in epileptogenic circuitry involving mesial temporal (limbic) structures, noting that bilateral limbic system pathology has been reported in TLE (e.g., reduced fractional anisotropy in the fornix and cingulum bilaterally)[56].

Our RF analyses demonstrated that a select set dFC features can effectively distinguish FBTCS+ as a whole from FBTCS− (see Table 6A, 70% classification accuracy), and current FBCTS+ status from remote FBTCS+ activity (see Table 6B, 78% classification accuracy). More specifically, our RF models revealed that a cardinal dFC feature of FBTCS+ involved heightened within subsystem dFC (recruitment) in select cortical (right DAN) and subcortical (left anterior thalamus) subsystems, as well as a specific elevated integrations between the left caudate and right cerebellar (cereb5) regions with the left VAN. A systematic review and meta-analysis of the brain network organization of focal epilepsy has reported a general pattern of increased network segregation during the interictal state[57]. The midline thalamus has been implicated in the propagation of temporal lobe seizures[58], but ours is the initial report of increased dFC among regions within the thalamus. While abnormally increased network homogeneity has been found in the right DAN in RTLE, our RF model highlighted the heightened dFC in the contralateral DAN of the FBTCS+ patients, a finding consistent with the expected widespread, contralateral impact of FBTCS+ activity. Through our data we also provided the initial report in LTLE of a heightened cortical/subcortical communication pattern involving two subcortical structures (the ictal caudate, the non-ictal cerebellum) with the cortical left VAN, noting that abnormal network homogeneity in the VAN network has been reported in right temporal lobe epilepsy[59]. As subcortical outputs from the caudate and cerebellum to thalamocortical circuits tend to be inhibitory[60], these increased integration findings in FBTCS+ may reflect communications aimed at breaking down inhibitory circuits, allowing for the spread of seizures. In addition, as our data reflected activity during the tonic resting state, our results indicated the pathologic signaling that supports FBTCS activity goes on outside of clinically observable FBTCS+ activity.

The only cortical networks with significant classification power were the attention networks, the DAN and VAN. Both the latter pointed to the potential neurocognitive impact of FBTCS activity. To examine this further, we tested on a post hoc basis the association between these features of FBTCS+ status and behavioral measures of attention (see supplementary text, p.25). Indeed, higher integration between the left caudate/left VAN were associated with higher levels of visual and auditory attention and slower information processing speed. As the VAN is specifically associated with stimulus-driven aspects of attention, including the reorienting of attention to unexpected or salient (e.g., target) stimuli (see[61,62]), this finding suggested that the presence of periodic FBTCS activity reinforced and increased attentional vigilance for these unpredictable seizure events. These correlations are also consistent with other data showing that brain network disorders such as epilepsy slow information processing speed[63,64].

Interestingly and surprisingly, only one feature discriminating the FBTCS+ /− groups belonged to the thalamic system. Prior reports of FBTCS+ /− group differences involved static network measures of the thalamus[5,20] or structural connectivity measures[65]. Accordingly, our data clarified that the dynamic connectivity perturbations brought on by FBTCS activity are predominantly within the thalamus, with evidence that the time invariant

disruptions to subcortico–cortico connectivity brought on by FBTCS activity involved other subcortical regions (i.e., striatum, cerebellum). Furthermore, there was limited representation in our FBTCS+ data of mesial temporal dFC. This is consistent with our expectations that the FBTCS+/− groups would show equivalence in the dFC features of the mesial temporal lobe because of shared pathology in that region. Importantly, consistent with our expectations that FBTCS activity is not limited to the ictal hemisphere. Our data demonstrated that the dFC abnormalities most characteristic of FBTCS+ involved prominent contralateral effects, most commonly increased recruitment (e.g., right DAN) and increased integration with cortical systems (e.g., right cerebellar with left VAN).

Our results, however, differ from the recent study by Hsieh et al.[35]. Hsieh and colleagues reported network features that distinguished generalized epilepsy patients (GE-GTCS) from those with focal epilepsy plus FBTCS (FE-FBTS) activity. They found the connectivity between cortex and thalamus were increased in GE-GTCS and decreased in FE-FBTS. They also found that compared with GE-GTCS, the cerebellar connectivity in FE-FBTS was increased when analyzing connectivity statically, and decreased when analyzing connectivity dynamically. In addition, the connectivity between the cortex and the thalamus was decreased overall in FE-FBTS[35]. The differences between the findings of Hsieh et al.[35] and our current study might have emerged from the fact that they utilized a different parcellation scheme and a dynamic analysis method based solely upon deviations across time windows (n.b., we utilized average correlations across all regions). In contrast, our dFC measures kept track of specific changes in network community membership and utilized a broader set of subcortical/cortical regional connectivities (n.b., the work of Pang et al.[66] differs from our study in similar ways).

We found that there were select cortical/subcortical integrations that appeared more characteristic of FBTCS+ current than remote status (e.g., left caudate with the left Control network; left cereb5 with left DMN). Heightened connectivity within the left anterior thalamus (recruitment) was also a feature distinguishing the FBTCS+ current group. The ipsilateral nature of these dFC features suggested that the impact of FBTCS activity may be time limited, with current seizure activity primarily impacting ipsilateral dFC. The correlational data with clinical epilepsy measures, however, were quite limited. For instance, the left cereb-5/left DMN integration feature bore no reliable association with age of seizure onset, but longer illness duration was associated with higher left cereb-5/left DMN integration in the FBTCS+ current group.

Lastly, the dFC features in the FBTCS+ remote group were ipsilateral in nature (left caudate/left Control integration) and these features were associated with older age of seizure onset and shorter illness duration.

Through our RF models we found the dFC features that best distinguished between FBTCS+/− and FBTCS+ current/remote status. We then investigated whether any of these features were related, raising the possibility that these systems do not operate independently in their implementation of FBTCS activity. Overall, these dFC measures showed few significant associations, suggesting a strong degree of independence among the networks impacting FBTCS activity. The only notable correlation involved higher left anterior thalamus recruitment (a feature important both for the classification of FBTCS+/− and FBTCS+ current/remote status), and two indications of higher integration (higher right cereb 5/left VAN; left cereb 5/left DMN). These correlations indicated highly selective dFC features do have inter-dependency, potentially revealing that there are small number of joint maladaptive subcortico–cortico connectivity effects playing a role in the development of FBTCS activity.

Several methodological considerations are relevant to this study. First, the sample size was relatively small, reducing power and increasing the chance of type II error especially for our LTLE subgroup analyses. Second, our data was completely silent as to whether the alterations in subcortical/cortical integrations reported for LTLE (or FBTCS) reflected alterations in anatomical connectivity. Third, the window length and sliding steps utilized in our dFC calculations were based upon prior published work by our group[54], where validations of the analytic pipeline (e.g., alterations in number of time windows and window length) were undertaken and parameters optimized. Nonetheless, the selection of window length and sliding steps may still have influenced our measures of network dynamics[67]. Fourth, it is noteworthy that AEDs can influence the blood oxygen level-dependent signal[68–70] and this may have influenced TLE/HP differences. Unfortunately, AED regimen heterogeneity (type, dosage, number of AEDs) and low sample sizes precluded further testing of these effects.

While there have been previous multilayer network studies in epilepsy that provided a context for our work, these studies focused on single subcortico–cortico system interactions[15,54,71]. Importantly, ours is the first report of the dynamic network connectivity (communication) alterations in multiple subcortico–cortico intrinsic systems in LTLE. We uncovered in LTLE both specialized subsystem communication between distal regions (integration effects), as well as more isolated communication within subsystems [recruitment, flexibility effects]. Our analyses also revealed several dynamic functional connectivity abnormalities unique to LTLE patients with FBTCS activity.

First, it is worth noting that through our analyses several normative hemispheric intrinsic connectivity dynamics emerged. Accordingly, we provided the first report that intrinsic dynamics within select subcortical (higher right than left anterior thalamic recruitment; higher left than right caudate and posterior hippocampal recruitment) and cortical systems (higher left than right hemisphere Visual, Somatomotor, VAN recruitment; DMN higher left than right) are not balanced across the hemispheres. Normative hemispheric biases in our dFC measures of flexibility were also evident (Limbic and DAN left biased; Somatomotor right biased). Our integration data demonstrated that intra-, not cross-hemispheric subcortical/cortical communication was normative, with several systems showing this pattern (thalamo/cortical, mesial temporal/cortical, striatum/cortical).

Regarding the dFC characteristics unique to LTLE, we revealed the flexibility of dFC among subcortical/cortical systems was generally higher in the hemisphere contralateral to the seizure. Also, in contrast to the normative ipsilateral integration pattern noted above as normative, a clear pattern of abnormal cross-hemispheric integrations was evident in LTLE (e.g., posterior thalamus/cortical; mesial temporal/cortical; putamen/Limbic).

While our data did not isolate one particular integration dFC as most abnormal in LTLE, the subcortical systems involved in these abnormal integrations with cortex all involved structures that have been implicated in the generation (hippocampus) or spread (thalamus, striatum) of epileptiform signals in TLE. This was consistent with our hypothesis that focal LTLE, irrespective of the FBTCS+ status, has a selective impact on multiple intrinsic subcortico–cortico communication systems in the brain. Prior rsFC work from our lab has shown the thalamus and striatum to be important to seizure generalization related to loss of a "braking function" on seizure propagation (see[20,45] for thalamus; see[5] for basal ganglia). It is important to note that these prior reports involved static measures of functional connectivity. Accordingly, our new findings demonstrated that additional sets of abnormal dynamic subcortical-cortical integrations are present in the tonic resting state in LTLE[5,20,45], clarifying that these time variant integration abnormalities are largely cross-hemispheric in nature.

Our RF models revealed a set of striatum-cortico and cerebellar-cortico communication pathways that appeared to be cardinal features of FBTCS+ compared to FBTCS− status, noting that the striatum and cerebellum house important motor output functionalities of the type that one sees in FBTCS[60]. More specifically, FBTCS+ patients displayed increased recruitment in both cortical (contralateral DAN system) and subcortical (ipsilateral anterior thalamus) subsystems, in addition to increased integration of both left caudate and right cereb5 with left VAN. As the FBTCS+ dynamic abnormalities reported here emerged from a baseline inter-ictal state, our data demonstrated that there were widespread abnormal intra-subcortical and subcortico-cortical communications present outside of clinically observable tonic–clonic seizure activity. Important differences emerged regarding when the FBTCS+ activity occurred. Current FBTCS activity perturbed dynamics more strongly than remote activity, with a separate set of heightened within thalamic subsystem dFC (increased recruitment) and striatum-cortico and cerebellar-cortico integrations unique to current compared to remote FBTCS+ status.

Consistent with our hypothesis, we observed that dFC metrics showed multiple abnormalities in subcortico–cortico dFC in LTLE as a whole and specifically in relation to FBTCS activity. Interestingly, RF models revealed no dFC integrations involving the thalamus with cortex. The FBTCS+ thalamic abnormalities we observed solely involved heightened, changing communications restricted to (within) thalamic regions, with these abnormalities not perturbing cortical dynamics. Thus, our dFC data implied that the thalamic/cortical connectivity abnormalities reported in the literature may arise from the use of static or time invariant functional connectivity measures[5,20]. Note, our data did indicate that FBTCS+ activity puts focal TLE patients at risk for more widespread brain dynamic functional connectivity disruptions, but these involved the striatum and cerebellum, not the thalamus. In this regard, we noted that some of the integration abnormalities of FBTCS+ (left caudate/left VAN, right cereb5/left VAN) were associated with alterations in attention (heightened vigilance) and slower information processing speed, suggesting motor and attention system communications are dysregulated in this group.

Our data on the association of dFC integrations across systems indicated that as the brain dynamically reconfigures in response to generalized seizures the cortical/subcortical systems do not respond in global or unified way. Instead, the systems generally showed a strong degree of independence. The implication is that the production of FBTCS+ activity does not require broad cooperation or joint activity between different coordinated subcortical/cortical systems. There was one notable exception (i.e., left anterior thalamic recruitment was correlated with higher integration between the cerebellum and VAN and DMN), indicating that select drivers of maladaptive FBTCS may develop in a concurrent fashion, potentially suggesting some joint effects do play a role in the development of FBTCS activity. This will require further study.

Overall, our data demonstrated that the baseline, inter-ictal state provides a breeding ground that reconfigures functional organization and communication both within multiple subcortical systems, and between multiple cortical and subcortical systems. These reconfigurations reflected both the proximal and distal specialized pathologic systems generated by epileptogenic activity in LTLE regardless of FBTCS status. Importantly, unique dFC abnormalities were present in focal TLE patients with FBTCS activity. While there did not appear to be one specific subcortical system dominating the interactions with cortex, integrations involving the caudate and cereb-5 subcortical subsystem were most common. As these structures are established parts of motor output circuitry it seems reasonable that they would provide the underpinnings of FBTCS motor activity. Thus, the network disruptions we report clarify the substrates that form the neurobiological basis of seizure generalization in focal TLE. Our data made clear that these subcortical-cortical integrations are not constant and static, but reflect transient perturbations, a feature that aligns with the intermittent nature of FBTCS activity. The dFC abnormalities reported here should be studied to further clarify if they can serve as early biomarkers of the functional connectivity changes that mark the transition from focal seizures to the more severe form of the disorder (FBTCS +). In this sense, our findings have prognostic value as they point to the formation of epileptogenic networks that place patients at risk for FBTCS activity, providing information that would encourage prophylactic medication strategies. Similarly, as such networks would be untouched by TLE surgery, their disruption would alter predictions about surgical outcome.

Methods
Participants
A total of fifty-five patients with refractory focal left TLE (LTLE) were recruited from the Thomas Jefferson Comprehensive Epilepsy Center. All patients were surgical candidates for either a standard anterior temporal lobectomy or thermal ablation of the ictal mesial temporal lobe, determined by a multimodal evaluation including neurological history/examination, scalp video-EEG, MRI, PET, and neuropsychological testing[72] (See Supplementary text, p.4 for more details). All patients had focal impaired awareness seizures (FIAS) and/or FAS (focal aware seizures), and a sub-sample had additional FBTCS. For our analyses, patients were classified into three groups based on their history at the time of scanning: (i) patients who had never had any FBTCS events during their lifetime (FBTCS−, n = 15); (ii) patients who had a remote history of FBTCS, but none within a

year of scanning (FBTCS+ remote group, n = 13); and (iii) patients who had recurrent FBTCS within the year prior to scanning (FBTCS+ current group, n = 27). A total of 56 age-, and gender-matched right-handed healthy participants (HPs) were also recruited (see Table 1 for sample demographic and clinical characteristics). All HPs were free of psychiatric or neurological disorders based on a health screening measure. The study was approved by the Ethics Committee of the Thomas Jefferson University and was conducted in compliance with the Declaration of Helsinki. All study participants provided written informed consent.

Imaging data acquisition and preprocessing of resting state data

All participants underwent a structural scan along with an 8 min resting state functional MRI scan (Philips 3 T) in which the participants viewed a crosshair with no task requirements. fMRI data collection and processing was identical to our prior work (see[73] and supplementary text, p. 4). In detail, the fMRI data was collected with a single shot echoplanar gradient echo imaging (EPI) sequence acquiring T2* signals (192 volumes; 34 axial slices acquired parallel to the anterior, posterior commissure line; TR = 2.5 s, TE = 35 ms; FOV = 256 mm, 128 × 128 data matrix voxels, flip angle = 90°, in-plane resolution = 2 mm × 2 mm, slice thickness = 4 mm). The structural T1-weighted and fMRI data were pre-processed using fmriprep 20.2.4 pipeline, which is the best software implementation of state-of-the-art protocols for the preprocessing of functional MRI data[74]. Each EPI imaging series started with three discarded scans to allow for signal stabilization (see Supplementary text for details on data preprocessing, p.4 and 5). Of note, subjects with more than 10% of outlier volumes (frame-wise displacements[75]; Derivatives of rms VARiance over voxelS[76] during the fMRI scan were excluded from analyses. All the participants in the study (55 left TLE group and 56 healthy normals) satisfied this criterion (7 subjects from the initially recruited 62 TLE patients and 4 from the initially recruited 60 healthy participants did not satisfy this criterion and, therefore, were excluded from the analyses). Prior to collection of the T2* images, T1-weighted images (180 slices) were collected using an MPRAGE sequence (256 × 256 isotropic 1 mm voxels; TR = 640 ms; TE = 3.2 ms, FOV = 256 mm, flip angle = 8°) in positions identical to the functional scans to provide an anatomical reference. The in-plane resolution for each T1 slice was 1 mm^3 (axial oblique).

Identification of cortical and subcortical networks

In order to define various cortical networks, we utilized the 200 cortical parcels in the Schaefer atlas to define seven intrinsic cortical networks (ICN's: Visual [VIS], Somatomotor [SMN], Dorsal Attention Network [DAN], Ventral Attention Network [VAN], Limbic [LIM], Executive Control [EC], Default Mode Network [DMN])[53]. These seven networks are more homogeneous than the four network version previously published[46], and are widely utilized and well-established in the neuroimaging literature. In our analyses, the left- and right-hemisphere aspects of each ICN were considered separately. We defined three subcortical systems using the 54 subcortical regional parcellation of the human subcortex as defined by Tian et al[47]. We divided the 54 parcels into the left–right mesial-temporal system (anterior and posterior hippocampus, and amygdala), left–right striatal system (putamen, caudate, globus palludus, nucleus accumbens), and the left–right thalamic system (anterior and posterior thalamus). The cerebellar systems were obtained using the 7-network cerebellar parcellations by Buckner et al[48], broken down by cerebellar hemisphere.

Network construction

The Supplement text provides detailed methodology. Key network construction steps included the following. Head motion influence was regressed out from the preprocessed functional MRI data by utilizing: (1) signals from aCompCor components, the first 5 components each corresponding to white matter and CSF masks, (2) 24 motion parameters, their temporal derivatives, and quadratic terms of both, (3) outlier frames with FD > 0.5 mm and DVARS (Derivative of rms VARiance over voxelS) with a threshold of ± 3 SD, together with their temporal derivatives, and (4) linear trend. Denoised functional data files were parcellated into 268 regions of interest (200 cortical, 54 subcortical and 14 cerebellar parcellations). Out of the 268 parcels, the BOLD signal from the parcels corresponding to the thalamus/7 cortical networks, striatum/7 cortical networks, mesial temporal/7 cortical networks and cerebellum/7 cortical networks were extracted (Fig. 1A). A wavelet decomposition was applied to extract information in the frequency interval of 0.05–0.1 Hz (scale 2)[77]. A sliding-window approach (length/step = 40/20 s, 23 windows in total) was applied to parse the decomposed time-series. Wavelet coherence was then used to estimate the adjacency matrix for each window and coupled all 23 windows into a multilayer network[78,79].

Dynamic community detection

A multilayer community detection algorithm was applied on the resting state multilayer network of each participant to extract groups of brain regions (i.e. communities) that were functionally connected with one another at each layer (Supplement text for description of algorithm[49]).

Dynamic network statistics

Three dynamic network statistics were estimated for each dynamic community structure detected from each multilayer network to characterize the dFC within the four subcortical systems (recruitment, flexibility dFC measures), and the interaction between the four subcortical systems and seven cortical systems (flexibility, integration; see Supplement text).

Module allegiance

This measure was used to summarize the consistency with which the parcels of the subcortical and cortical systems were assigned to communities over time[50,55]. See supplementary text for details.

Flexibility, recruitment and integration

The subcortical parcels were grouped on the basis of their main anatomical boundaries into the following subsystems to finely probe pairwise functional interactions with the cortical networks (see Supplement text, Data Processing, p. 9): (1) thalamus—left/right anterior thalamus [5 parcels each] and posterior thalamus [3 parcels each], (2) striatum—left/right putamen [4 parcels each], caudate [4 parcels each], nucleus accumbens [2 parcels each] and globus pallidus [2 parcels each], (3) mesial temporal—left/right anterior hippocampus [3 parcels each], posterior hippocampus [2 parcels each] and amygdala [2 parcels each], and (4) cerebellum—left/right cereb1 to cereb7 [corresponding to 7Networks_1 to 7Networks_7 as defined by Buckner et al[48]]. The seven cortical networks (VIS, SMN, DAN, VAN, LIM, EC and DMN) were also divided into left and right hemisphere forms (subsystems), combining all the left and right hemispheric parcels of each system. The following measures of community membership change and interaction were analyzed: (1) *flexibility*, that captures the frequency with which a particular parcel changes its community assignment over time, (2) *recruitment*, that quantifies the probability with which each parcel in each of the cortical/subcortical subsystems was assigned to the same community as parcels from the same subsystem, (3) *integration*, that quantifies the probability with which each parcel in each cortical/subcortical system was assigned to the same community as parcels from the other subsystems over time[50,51,78].

Statistical analyses

To determine group differences in our dFC measures rmMANOVAs were conducted using MATLAB functions or IBM® SPSS® v23 with alpha level set at $p < 0.05$ for both multivariate and univariate effects with appropriate correction for multiple comparisons. Preliminary assumption testing checked for independence of observations, normality, and sphericity. Independence of observations and normality were met. If sphericity was violated, the Huynh–Feldt correction was applied (epsilon > 0.75) to determine significant univariate effects. Tables 2, 3, 4 and 5 present the significant univariate effects ($p < 0.05$ or less), with notations indicating if the multivariate test (Wilks' Lambda) was significant ($p < 0.05$ or less). Post hoc pairwise comparisons were applied to the significant univariate effects to delineate the nature of the finding.

In the rmMANOVAs on our three dFC measures (recruitment, flexibility, and integration, run separately) experimental group (HP/LTLE, FBTCS+/FBTCS−, or FBTCS+ current/remote) served as a between-subjects factor. Hemisphere (left ictal/right non-ictal) and subsystem (subcortical/cortical) served as within-subject factors. The rmMANOVAs on recruitment, flexibility, and integration were run separately, with separate models for the different subcortical/cortical combinations: thalamus with each of seven cortical, striatum with each of seven cortical, mesial temporal with each of seven cortical, and cerebellum with each of seven cortical; see supplement text (see Tables 2, 3, 4 and 5 for results). As per the definition, the dynamic measure of recruitment was calculated for each parcel of a subsystem as the probability with which it was assigned to the same community as other parcels from the same subsystem. The recruitment of the subsystem was then calculated as an average of the recruitment values of all constituent parcels. As the cerebellar subsystems in Buckner atlas[48] were not divided into finer grained parcels, we were unable to compute recruitment for those subsystems. The rmMANOVAs aimed to detect LTLE/HP differences and utilized the raw recruitment, flexibility, and integrations variables in each model. In the rm MANOVAs aimed at detecting FBTCS+ /FBTCS− or FBTCS+ current/remote differences, we utilized the dFC values of our matched HPs as a reference point, calculating the patient specific z-score deviation from the HPs with the following formula:

$$Z_{pat} = (dFC_{pat} - \mu_{con}) / \sigma_{con} \tag{1}$$

where μ_{con} and σ_{con} were the mean and standard deviation of the same dFC matrix from the HPs. These deviation scores were entered into the rmMANOVA models described above as the dependent variables (repeated measures factors), with the patient group comparison as the between subjects-factor (FBTCS+ /FBTCS−, FBTCS+ remote/current).

To capture and select the strongest predictors of FBTCS+ status, we leveraged the classification power of permutation-based Random Forest (RF) machine learning to select and rank the subcortical and cortical recruitment, flexibility, and integration features that emerged as significant in the FBTCS+ focused rmMANOVAs. More specifically, the inputs to our RF models (bootstrapping and cross validations) were the subcortical/cortical dFC parameters that yielded a significant subsystem X group, or hemisphere X subsystem X group interaction effects in the FBTCS+ rmMANOVAs. In the first RF classifier model, the FBTCS+ and FBTCS− groups served as the response or dependent measure. In the second RF classifier model, the FBTCS+ current and FBTCS+ remote groups served as the response measure. The RF output provided variable importance scores indicating the features most heavily weighted in the discrimination of the groups. An RF predictor variable meeting a 0.60 significance ratio criterion was a considered significant, reliable classifier in the model (n.b., significance ratio quantifies the proportion of times a variable was deemed significant, $p < 0.05$, out of the 500 repetitions; see details in Supplement text p. 11). The directional effect of a given predictor (i.e., which group possessed a higher significance ratio) was assessed from the univariate effects table associated with the relevant rmMANOVA analysis. Note, RF accounts for linear/non-linear effects, interactions, overfitting, high dimensionality (overcoming collinearity) without huge sample size requirements[80]. The RF process was run in a leave-one-out cross validation manner, such that the most important variables were identified and used to establish an RF model based on the n-1 training samples. This allowed us to classify the groups in the "left over" testing sample. These RF analyses and procedures were performed in MATLAB with in-house MATLAB codes[38]. To examine if the RF features with high variable importance scores were associated (i.e., showed dependency on one another), we ran Pearson correlations.

To determine if the strength of these associations (correlations) differed between the FBTCS+/− or the FBTCS+ (current/remote) groups we Fisher z-transformed the Pearson correlations and tested for group differences via an in-house python code. Lastly, to determine whether the RF features with high variable important scores were associated with measures of epilepsy history and seizure severity, we ran univariate Pearson correlations between the RF features and key clinical epilepsy variables (age of seizure onset and illness duration).

Data availability

The data that support the findings of this study are not openly available due to reasons of sensitivity and are available from the corresponding author upon reasonable request.

References

1. Vuong, J. & Devergnas, A. The role of the basal ganglia in the control of seizure. *J. Neural Transm. (Vienna, Austria: 1996)* **125**(3), 531–545 (2018).
2. Bartolomei, F. et al. Defining epileptogenic networks: Contribution of SEEG and signal analysis. *Epilepsia* **58**(7), 1131–1147 (2017).
3. Jobst, B. C. et al. Secondarily generalized seizures in mesial temporal epilepsy: Clinical characteristics, lateralizing signs, and association with sleep-wake cycle. *Epilepsia* **42**(10), 1279–1287 (2001).
4. Caciagli, L. et al. Thalamus and focal to bilateral seizures: A multiscale cognitive imaging study. *Neurology* **95**(17), e2427–e2441 (2020).
5. He, X. et al. Disrupted basal ganglia-thalamocortical loops in focal to bilateral tonic-clonic seizures. *Brain* **143**(1), 175–190 (2020).
6. Yoo, J. Y. et al. Ictal spread of medial temporal lobe seizures with and without secondary generalization: An intracranial electroencephalography analysis. *Epilepsia* **55**(2), 289–295 (2014).
7. Janszky, J. et al. Temporal lobe epilepsy with hippocampal sclerosis: Predictors for long-term surgical outcome. *Brain* **128**(Pt 2), 395–404 (2005).
8. Bone, B. et al. Secondarily generalized seizures in temporal lobe epilepsy. *Epilepsia* **53**(5), 817–824 (2012).
9. Keller, S. S. et al. Thalamotemporal alteration and postoperative seizures in temporal lobe epilepsy. *Ann. Neurol.* **77**(5), 760–774 (2015).
10. Lawn, N. D., Bamlet, W. R., Radhakrishnan, K., O'Brien, P. C. & So, E. L. Injuries due to seizures in persons with epilepsy: A population-based study. *Neurology* **63**(9), 1565–1570 (2004).
11. Walczak, T. S. et al. Incidence and risk factors in sudden unexpected death in epilepsy: A prospective cohort study. *Neurology* **56**(4), 519–525 (2001).
12. Harden, C. et al. Practice guideline summary: Sudden unexpected death in epilepsy incidence rates and risk factors: Report of the guideline development, dissemination, and implementation subcommittee of the American Academy of Neurology and the American Epilepsy Society. *Neurology* **88**(17), 1674–1680 (2017).
13. Fan, B. et al. Correlation between the functional connectivity of basal forebrain subregions and vigilance dysfunction in temporal lobe epilepsy with and without focal to bilateral tonic-clonic seizure. *Front. Psychiatry* **13**, 888150 (2022).
14. Nie, L. et al. A study of brain functional network and alertness changes in temporal lobe epilepsy with and without focal to bilateral tonic–clonic seizures. *BMC Neurol.* **22**, 14 (2022).
15. He, X. et al. Uncovering the biological basis of control energy: Structural and metabolic correlates of energy inefficiency in temporal lobe epilepsy. *Sci. Adv.* **8**(45), eabn2293 (2022).
16. Bertram, E. H., Zhang, D. & Williamson, J. M. Multiple roles of midline dorsal thalamic nuclei in induction and spread of limbic seizures. *Epilepsia* **49**(2), 256–268 (2008).
17. Bernhardt, B. C., Bernasconi, N., Kim, H. & Bernasconi, A. Mapping thalamocortical network pathology in temporal lobe epilepsy. *Neurology* **78**(2), 129–136 (2012).
18. Yang, L. et al. Localized shape abnormalities in the thalamus and pallidum are associated with secondarily generalized seizures in mesial temporal lobe epilepsy. *Epilepsy Behav.* **70**(Pt A), 259–264 (2017).
19. Chen, C. et al. Alterations in the hippocampal-thalamic pathway underlying secondarily generalized tonic-clonic seizures in mesial temporal lobe epilepsy: A diffusion tensor imaging study. *Epilepsia* **60**(1), 121–130 (2019).
20. He, X., Doucet, G. E., Sperling, M., Sharan, A. & Tracy, J. I. Reduced thalamocortical functional connectivity in temporal lobe epilepsy. *Epilepsia* **56**(10), 1571–1579 (2015).
21. Peng, S. J. & Hsin, Y. L. Altered structural and functional thalamocortical networks in secondarily generalized extratemporal lobe seizures. *Neuroimage Clin.* **13**, 55–61 (2016).
22. Guye, M. et al. The role of corticothalamic coupling in human temporal lobe epilepsy. *Brain* **129**(Pt 7), 1917–1928 (2006).
23. Blumenfeld, H. The thalamus and seizures. *Arch. Neurol.* **59**(1), 135–137 (2002).
24. Norden, A. D. & Blumenfeld, H. The role of subcortical structures in human epilepsy. *Epilepsy Behav.* **3**(3), 219–231 (2002).
25. Castro-Alamancos, M. A. Neocortical synchronized oscillations induced by thalamic disinhibition in vivo. *J. Neurosci.* **19**(18), 27 (1999).
26. Wichmann, T. & DeLong, M. *The Basal Ganglia in Principles of Neural Science* 5th edn. (McGraw-Hill Education, 2014).
27. Alexander, G. E., DeLong, M. R. & Strick, P. L. Parallel organization of functionally segregated circuits linking basal ganglia and cortex. *Ann. Rev. Neurosci.* **9**, 357–381 (1986).
28. Alexander, G. E., Crutcher, M. D. & DeLong, M. R. Basal ganglia-thalamocortical circuits: Parallel substrates for motor, oculomotor, prefrontal and limbic functions. *Prog. Brain Res.* **85**, 119–146 (1990).
29. Blumenfeld, H. et al. Cortical and subcortical networks in human secondarily generalized tonic-clonic seizures. *Brain* **132**(Pt 4), 999–1012 (2009).
30. Rektor, I., Kuba, R., Brázdil, M. & Chrastina, J. Do the basal ganglia inhibit seizure activity in temporal lobe epilepsy?. *Epilepsy Behav.* **25**(1), 56–59 (2012).
31. Aupy, J. et al. Cortico-striatal synchronization in human focal seizures. *Brain* **142**(5), 1282–1295 (2019).
32. Parmeggiani, A., Posar, A. & Scaduto, M. C. Cerebellar hypoplasia, continuous spike-waves during sleep, and neuropsychological and behavioral disorders. *J. Child Neurol.* **23**(12), 1472–1476 (2008).
33. Xu, H., Zhu, H., Luo, L. & Zhang, R. Altered gray matter volume in MRI-negative focal to bilateral tonic-clonic seizures. *Acta Neurol. Belg.* **121**(6), 1525–1533 (2021).
34. Salgado-Benítez, A., Briones, R. & Fernández-Guardiola, A. Purkinje cell responses to a cerebral penicillin-induced epileptogenic focus in the cat. *Epilepsia* **23**(6), 597–606 (1982).
35. Hsieh, H. et al. Distinct functional cortico-striato-thalamo-cerebellar networks in genetic generalized and focal epilepsies with generalized tonic-clonic seizures. *J. Clin. Med.* **11**(6), 1612 (2022).
36. Braun, U. et al. Dynamic reconfiguration of frontal brain networks during executive cognition in humans. *Proc. Natl. Acad. Sci. USA* **112**(37), 11678–11683 (2015).

37. Filippi, M., Spinelli, E. G., Cividini, C. & Agosta, F. Resting state dynamic functional connectivity in neurodegenerative conditions: A review of magnetic resonance imaging findings. *Front. Neurosci.* **13**, 657 (2019).

38. Hinds, W. et al. Pre-surgical features of intrinsic brain networks predict single and joint epilepsy surgery outcomes. *NeuroImage Clin.* **38**, 103387 (2023).

39. Davis, K. A. & Morgan, V. L. Network analyses in epilepsy: Are nodes and edges ready for clinical translation?. *Neurology* **96**(5), 195–196 (2021).

40. Sinha, N., Johnson, G. W., Davis, K. A. & Englot, D. J. Integrating network neuroscience into epilepsy care: Progress, barriers, and next steps. *Epilepsy Curr.* **22**(5), 272–278 (2022).

41. Li, R. et al. Disruption of functional connectivity among the subcortical arousal system and cortical networks in temporal lobe epilepsy. *Brain Imaging Behav.* **14**(3), 762–771 (2020).

42. Bassett, D. S. & Sporns, O. Network neuroscience. *Nat. Neurosci.* **20**(3), 353–364 (2017).

43. Tatum, W. O. I. V. Mesial temporal lobe epilepsy. *J. Clin. Neurophysiol.* **29**(5), 356–365 (2012).

44. Kullmann, D. M. What's wrong with the amygdala in temporal lobe epilepsy?. *Brain* **134**(Pt 10), 2800–2801 (2011).

45. He, X. et al. Presurgical thalamic hubness predicts surgical outcome in temporal lobe epilepsy. *Neurology* **88**(24), 2285–2293 (2017).

46. Schaefer, A. et al. Local-global parcellation of the human cerebral cortex from intrinsic functional connectivity MRI. *Cereb. Cortex* **28**(9), 3095–3114 (2018).

47. Tian, Y., Margulies, D. S., Breakspear, M. & Zalesky, A. Topographic organization of the human subcortex unveiled with functional connectivity gradients. *Nat. Neurosci.* **23**(11), 1421–1432 (2020).

48. Buckner, R. L., Krienen, F. M., Castellanos, A., Diaz, J. C. & Yeo, B. T. The organization of the human cerebellum estimated by intrinsic functional connectivity. *J. Neurophysiol.* **106**(5), 2322–2345 (2011).

49. Mucha, P. J., Richardson, T., Macon, K., Porter, M. A. & Onnela, J.-P. Community structure in time-dependent, multiscale, and multiplex networks. *Science* **328**(5980), 876–878 (2010).

50. Bassett, D. S., Yang, M., Wymbs, N. F. & Grafton, S. T. Learning-induced autonomy of sensorimotor systems. *Nat. Neurosci.* **18**(5), 744–751 (2015).

51. Mattar, M. G., Cole, M. W., Thompson-Schill, S. L. & Bassett, D. S. A functional cartography of cognitive systems. *PLoS Comput. Biol.* **11**(12), e1004533 (2015).

52. Oldfield, R. C. The assessment and analysis of handedness: the Edinburgh inventory. *Neuropsychologia* **9**(1), 97–113 (1971).

53. Yeo, B. T. T. et al. The organization of the human cerebral cortex estimated by intrinsic functional connectivity. *J. Neurophysiol.* **106**(3), 1125–1165 (2011).

54. He, X. et al. Disrupted dynamic network reconfiguration of the language system in temporal lobe epilepsy. *Brain* **141**(5), 1375–1389 (2018).

55. Chai, L. R., Mattar, M. G., Blank, I. A., Fedorenko, E. & Bassett, D. S. Functional network dynamics of the language system. *Cereb. Cortex* **26**(11), 4148–4159 (2016).

56. Concha, L., Beaulieu, C. & Gross, D. W. Bilateral limbic diffusion abnormalities in unilateral temporal lobe epilepsy. *Ann. Neurol.* **57**(2), 188–196 (2005).

57. van Diessen, E. et al. Brain network organization in focal epilepsy: A systematic review and meta-analysis. *PLoS ONE* **9**(12), e114606 (2014).

58. Romeo, A. et al. Early Ictal recruitment of midline thalamus in mesial temporal lobe epilepsy. *Ann. Clin. Transl. Neurol.* **6**(8), 1552–1558 (2019).

59. Li, D. B. et al. Abnormal ventral attention network homogeneity in patients with right temporal lobe epilepsy. *Eur. Rev. Med. Pharmacol. Sci.* **25**(4), 2031–2038 (2021).

60. Dacre, J. et al. A cerebellar-thalamocortical pathway drives behavioral context-dependent movement initiation. *Neuron* **109**(14), 2326–2338 (2021).

61. Jimenez, A. M. et al. Abnormal ventral and dorsal attention network activity during single and dual target detection in schizophrenia. *Front. Psychol.* **7**, 323 (2016).

62. Corbetta, M. & Shulman, G. L. Control of goal-directed and stimulus-driven attention in the brain. *Nat. Rev. Neurosci.* **3**, 201–215 (2002).

63. Ferrario, R. & Giovagnoli, A. R. Processing speed in temporal lobe epilepsy: A scoping review. *Epilepsy Behav.* **142**, 109169 (2023).

64. McMillan, T. M., Mason, C. A., Seidenberg, M., Jones, J. & Hermann, B. The impact of processing speed on cognition in temporal lobe epilepsy. *Epilepsy Behav.* **122**, 108203 (2021).

65. Ge, Y. et al. Altered structural network in temporal lobe epilepsy with focal to bilateral tonic-clonic seizures. *Ann. Clin. Transl. Neurol.* **11**(9), 2277–2288 (2024).

66. Pang, L. et al. Disruption of cerebellar-cerebral functional connectivity in temporal lobe epilepsy and the connection to language and cognitive functions. *Front. Neurosci.* **16**, 871128 (2022).

67. Telesford, Q. K. et al. Detection of functional brain network reconfiguration during task-driven cognitive states. *Neuroimage* **142**, 198–210 (2016).

68. Jansen, J. F. et al. Functional MRI reveals declined prefrontal cortex activation in patients with epilepsy on topiramate therapy. *Epilepsy Behav.* **9**(1), 181–185 (2006).

69. Haneef, Z., Levin, H. S. & Chiang, S. Brain graph topology changes associated with anti-epileptic drug use. *Brain Connect.* **5**(5), 284–291 (2015).

70. Wandschneider, B. et al. Effect of topiramate and zonisamide on fMRI cognitive networks. *Neurology* **88**(12), 1165–1171 (2017).

71. Khambhati, A. N. et al. Dynamic network drivers of seizure generation, propagation and termination in human neocortical epilepsy. *PLoS Comput. Biol.* **11**(12), e1004608 (2015).

72. Sperling, M. R., O'Connor, M. J., Saykin, A. J. & Plummer, C. Temporal lobectomy for refractory epilepsy. *JAMA* **276**(6), 470–475 (1996).

73. Modi, S. et al. Multiple brain systems dynamically interact during tonic and phasic states to support language integrity in temporal lobe epilepsy. *Neuroimage Clin.* **32**, 102861 (2021).

74. Esteban, O. et al. fMRIPrep: A robust preprocessing pipeline for functional MRI. *Nat. Methods* **16**(1), 111–116 (2019).

75. Jenkinson, M., Bannister, P., Brady, M. & Smith, S. Improved optimization for the robust and accurate linear registration and motion correction of brain images. *Neuroimage* **17**(2), 825–841 (2002).

76. Power, J. D., Barnes, K. A., Snyder, A. Z., Schlaggar, B. L. & Petersen, S. E. Spurious but systematic correlations in functional connectivity MRI networks arise from subject motion. *Neuroimage* **59**(3), 2142–2154 (2012).

77. Percival, D. B. & Walden, A. T. *Wavelet Methods for Time Series Analysis* (Cambridge University Press, 2000).

78. Bassett, D. S. et al. Dynamic reconfiguration of human brain networks during learning. *Proc. Natl. Acad. Sci. USA* **108**(18), 7641–7646 (2011).

79. Braun, U. et al. Dynamic brain network reconfiguration as a potential schizophrenia genetic risk mechanism modulated by NMDA receptor function. *Proc. Natl. Acad. Sci. USA* **113**(44), 12568–12573 (2016).

80. Altmann, A., Toloşi, L., Sander, O. & Lengauer, T. Permutation importance: A corrected feature importance measure. *Bioinformatics* **26**(10), 1340–1347 (2010).

Author contributions

SM: Conceptualization, Methodology, Investigation, Writing – original draft. AA: Investigation. WH: Investigation. MRS: Investigation. XH: Investigation. JIT: Conceptualization, Methodology, Investigation, Writing – original draft, review and editing, Supervision.

Declarations

Competing interests

The authors declare no competing interests.

Additional information

Supplementary Information The online version contains supplementary material available at https://doi.org/10.1038/s41598-025-96418-4.

Correspondence and requests for materials should be addressed to J.I.T.

Reprints and permissions information is available at www.nature.com/reprints.

Publisher's note Springer Nature remains neutral with regard to jurisdictional claims in published maps and institutional affiliations.